Analysis of Beam Properties of Lorentz-Gauss and Hermite-Gaussian beams for Unstable Resonator through Paraxial ABCD Optical System

Dissertation Submitted towards the partial fulfillment of requirement for the award of degree of

Master of Engineering

In

Electronics and Communication Engineering

Submitted by:

Nivedita Mishra

(801361019)

Under the guidance of:

Dr. Hardeep Singh

(Assistant Professor)

ELECTRONICS AND COMMUNICATION ENGINEERING DEPARTMENT

THAPAR UNIVERSITY

(Established under the section 3 of UGC Act, 1956)

PATIALA – 147004 (PUNJAB)

DECLARATION

I hereby declare that the work presented in this dissertation entitled as "**Analysis of Beam Properties of Lorentz-Gauss and Hermite-Gaussian beams for Unstable Resonator through Paraxial ABCD Optical System**" is an authentic record of my study carried out as partial fulfillments of the requirement for the award of degree of Master of Engineering (Electronics and Communication Engineering) at Thapar University, Patiala, under the supervision of Dr. Hardeep Singh.

I have not submitted the matter presented in this thesis for the award of any other degree of this or any other university.

Date: 07/07/15

Nivedita Mishra
(801361019)

It is certified that the above statement made by the student is correct to the best of my knowledge and belief.

Date: 07/07/15

Dr. Hardeep Singh
Assistant Professor, ECED

Countersigned by:

Dr. Sanjay Sharma
Professor and Head, ECED
Thapar University, Patiala

Dr. S S Bhatia
Dean of Academic Affairs
Thapar University, Patiala

i

ACKNOWLEDGEMENT

First of all, I would like to express my gratitude to **Dr. Hardeep Singh, Assistant Professor**, Electronics and Communication Engineering Department, Thapar University, Patiala for his patient guidance and support throughout this report. I am truly very fortunate to have the opportunity to work with him. I found this guidance to be extremely valuable.

I am also thankful to our **Head of Department, Dr. Sanjay Sharma** as well as **PG Coordinator, Dr. Amit Kumar Kohli, Associate Professor**, of Electronics and Communication Engineering Department. I would like to thank entire faculty and staff of Electronics and Communication Engineering Department and then friends who devoted their valuable time and helped me in all possible ways towards successful completion of this work. I thank all those who have contributed directly or indirectly to this work.

Lastly, I would also like to thank my parents for their years of unyielding love and encouragement. They have always wanted the best for me and I admire their determination and sacrifice.

Date: 21/06/2015 Nivedita Mishra

Place: Patiala (801361019)

ABSTRACT

Light can take the form of beams that are an approximate version of waves which are spatially localized and non-divergent. Waves with wave front normal making small angles with z-axis are called paraxial waves. These waves must satisfy the Helmholtz equation. This equation has important applications in the science of optics, where it provides solutions that describe the propagation of electromagnetic waves (light) in the form of either paraboloidal waves or Gaussian beams. Most lasers emit beams that take this form. The solution of this equation shows the characteristics of an optical beam called as Gaussian beam. Our focus is on the beams which have the wave front similar to Gaussian beam i.e. paraboloidal wave front but with different intensity distribution. Beams with paraboloidal wave front match the curvatures of spherical mirror with large radius.

Advances in nanometer technology have triggered a broad activity in low-dimensional quantum systems. It started with two-dimensional (2D) electron systems at the interface of two materials several decades ago, and recently it has shifted to 2D materials, for example, 2D topological insulators, and graphene. The most interesting feature of these systems is their similarity to ultrarelativistic electrons and positrons which obey the Dirac equation. In photonics an intermediate approach has been widely used which is based on beam optics, in particular, in laser physics. Ray optics with the inclusion of essential phenomena such as diffraction and interference gives the base for Beam optics. Compared to mechanics it corresponds to the quasi-classical approach. For the case of electromagnetic phenomena, the meta-material properties of p-n junctions in graphene can be understood by inspecting classical trajectories or using ray optics.

In this work we have compared the characteristics of Effective beam size and Spatial complex degree of coherence of Lorentz-Gauss beam and Hermite-Gaussian beams. The mathematical model of Lorentz-Gauss beam and Hermite-Gaussian beam is analyzed in terms of *ABCD* parameters. The dependence of Effective beam size and Spatial complex degree of coherence on beam parameters and coherence length is shown and the role of *ABCD* parameters is widely discussed.

We have found out in this work that for effective beam size of Lorentz-Gauss beams there exists a threshold point between coherence length value of 0.1 mm to 2 mm. In contrast to Lorentz-Gauss beams where there is a threshold point after which effective beam size is asymptotically increasing for Hermite-Gaussian beams there exists a threshold point after which effective beam size diminishes. The Spatial complex degree of coherence is found out to be same for both the beams. In this work the effect of beam parameters on effective beam size is shown for unstable resonator.

The results obtained will be useful in long-distance Optical communication. The approach used in this work can be extended in the field of photonics.

Table of Contents

List of Figures

List of Tables

CHAPTER 1

Introduction to Optical Beams

1.1 Basics

Optical communication uses light to carry information for transmission at a distance. It can be used visually or by using electronic devices. Most common type of channel is optical fiber. The transmitters in optical communication are light emitting diode, Lasers. Infrared light is used more frequently due to the inherent property of optical fibers to transmit infrared light with minor attenuation and dispersion then visual light. Light can take the shape of beams that are an approximate version of waves which are spatially localized and non-divergent. Waves can be defined as spherical and plane waves based on the wave fronts. The wave fronts in plane waves form parallel planes that are travelling in same direction, perpendicular to plane's surface. A spherical wave is generated by a point like source, with the spherical wave fronts spreading radially outward from the point source.

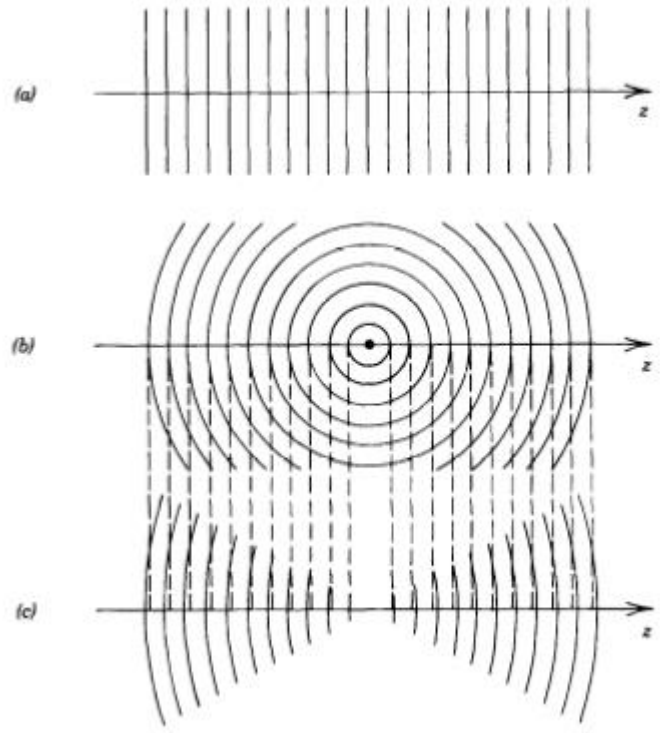

Figure 1.1 (1)-Wave front of uniform plane wave, (2)-Wave front of spherical wave, (3)-Wave front of Gaussian beam [1]

1.2 Gaussian Beam

Waves with wave front normal making small angle with respect to z axis are referred to as paraxial waves. These waves have to follow Helmholtz equation. The result of this equation shows the features of an optical beam referred to as Gaussian beam. This intensity distribution when investigated in any arbitrary transverse plane is Gaussian function which is circularly symmetric and is focused about beam axis. This beam width of Gaussian distribution is minimal on its beam waist and advances steadily in the two directions. Wavefronts are almost constant closer to beam waist, and they regularly bend and turn out to be generally sphere-shaped away from waist. For a presumed beam width these beams exhibit the minimum angular divergence for wavefront normals allowed by the wave equation. The wave front normal can be seen as a slender pencil of rays. In the optimal environment, light emitting from laser beam proceed to convert to the shape of Gaussian beam. It is one of the most important beams in optical communication; properties of beams are defined taking Gaussian beam as fundamental beam.

1.3 Properties of Gaussian Beams

1.3.1 Wave fronts

The component defined in phase of Gaussian beam as

$$\frac{K\,(p^2)}{[2\ \times\ R\,(z)]}$$

is the term responsible for bending of wave front. It shows the divergence of phase on off axis points in specified transverse plane from the axial point.

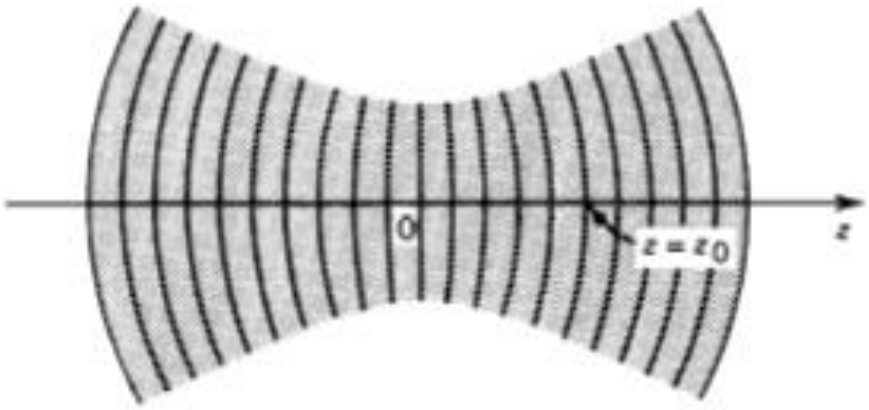

Figure 1.2 Wave front of a Gaussian beam [1].

1.3.2 Intensity

The optical intensity depends on optical and radial distance. On each point of axial distance intensity is found out to be Gaussian function of radial distance therefore the beam is named as Gaussian beam. This Gaussian term has its zenith on the beam axis i.e. at zero radial distance and its value decreases monotonically with the increase in radial distance. Along with this change in peak value, width of this allocation increase with axial distance.

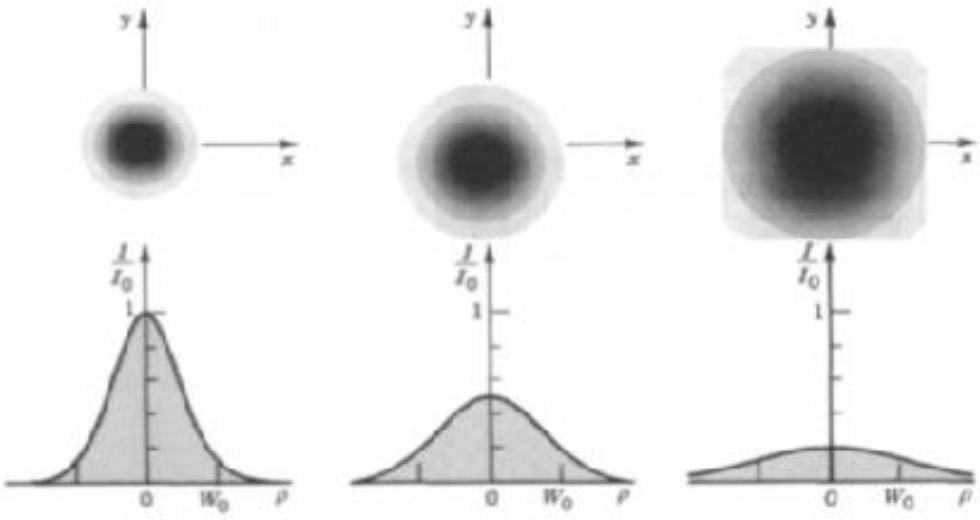

Figure 1.3 The normalize beam intensity I/I_0, as function of radial distance on different axial distance (1) z=0, (2) $z=z_0$, (3) $z=2z_0$ [1].

1.3.3 Power

The overall optical power of a beam is defined in terms of optical intensity and it is equivalent to integration of optical intensity over given plane. Hence, the beam power is obtained as beam area multiplied by half of beam intensity.

1.3.4 Beam Divergence

The beam divergence is defined as,

$$\Theta = (2/\pi)*(\lambda/2*W_0)$$

It clearly shows that beam divergence is directly proportional to wavelength and is inversely proportional to spot size or beam waist diameter. If waist size shrinks, beam

gets diverged hence we must use a smaller wavelength and larger beam waist so that beam converges [1].

1.3.5 Beam Radius

In a Gaussian function the beam intensity is maximum at beam axis and it decreases with increase in radial distance. The beam intensity falls by the factor $1/e^2$, which is equal to 0.135 for a radial distance say W(z). This circle formed using the distance W(z) as radius confines 86% of power in itself and this radius W(z) is referred to as beam radius or beam width. Its minimum value W_0 is found in source plane z=0, this value is called as Beam Waist. This value W_0 is called as Waist Radius and $(2 \times W_0)$ is called as Spot Size.

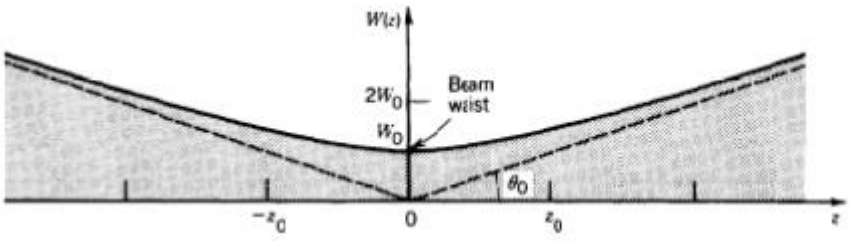

Figure 1.4 Radius of beam W(z) possesses smallest value at z=0, at $z=\pm z_0$ reaches $\sqrt{2}W_0$ and then increase linearly with z [1].

1.3.6 Phase

Phase of Gaussian beam is defined as;

$$\Phi(p, z) = k \times z - b(z) + \left[\frac{k(p^2)}{2 \times R(z)}\right]$$

On the beam axis the phase changes to:

$$\Phi(0,z) = (k \times z) - b(z)$$

This equation is comprised of two components: One component is $(k \times z)$ and it denotes phase of plane wave. Other component denotes phase retardation factor b(z), its range is between $-\pi/2$ at $z = -\infty$ to $+\pi/2$ at $z = \infty$. The phase retardation is the excess delay as compared with plane or spherical wave. It is clear that total excess phase retardation in wave when it propagates from $z = -\infty$ to ∞ is 'π'.

The Guoy phase shift shows that as Gaussian beam passes from focus, it picks up additional phase shift π, with the usual e^{-jkz} phase shift which is likely from plane wave. This occurrence is known as 'Guoy Effect' [1].

1.3.7 Depth of Focus

The minimum width of beam is seen at z=0 plane. In other directions i.e. in both the sides of z=0 beam starts being 'out of focus'. The axial distance where beam radius lies with a factor of $\sqrt{2}$ of the minimum beam radius value is called as 'Depth of Focus' and it is also known as 'Confocal parameter'.

The Confocal parameter is directly proportional to area of beam at beam waist and is inversely proportional to wavelength. Hence, it can be concluded that if a beam is fixed to minute spot size, depth of focus will be short and the plane of focus should be placed with larger precision in this case.

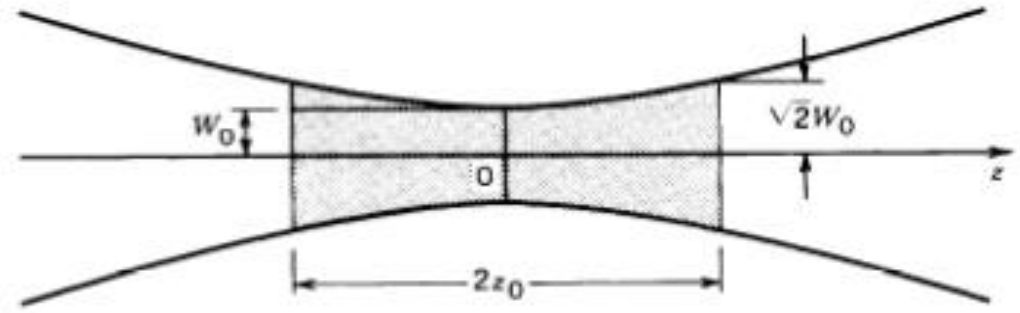

Figure 1.5 Confocal Parameter of a Gaussian beam [1]

1.4 Importance of Gaussian Beam

- Modes of spherical resonator are given by Gaussian beams so these are formed logically by lasers.
- Gaussian beam do not change its properties while passing through an optical element it remains Gaussian.
- Single mode lasers have beam profile very close to Gaussian beam.

- Beam propagation factor; M^2 factor is a generalized factor for analysing the beams whose beam quality is poor, this analysis is the Gaussian mode analysis. It is used to quantify quality of beam of laser.
- M^2 factor is equal to unity for Gaussian beam and for all the real laser beams this value is greater than one; though some higher quality beams possesses this value close to unity such as Lorentz beam.

1.5 Optical Beams

Light can take the form of beams and according to our need we can use one; there are several kind of beams some of our special concern are discussed in this section.

Hermite Gaussian Beam (HGB)

Gaussian beams are not the single possible solution of Helmholtz equation; there are some other possible solutions whose intensity distribution is non Gaussian. Our area is up to those beams which have the wave front similar to Gaussian beam i.e. paraboloidal wave front but with different intensity distribution. Beams with paraboloidal wave front equate the curvature of spherical mirror with bigger radius. Hence these types of beams can replicate amid two spherical mirrors which form resonator without being distorted. They are self producing waves and are referred to as resonator modes.

Laguerre Gaussian Beam

Hermite Gaussian beam forms a whole set of solution for Helmholtz equation but it is not the only possible set of solution, Laguerre Gaussian beam also form the whole set of solution for Helmholtz equation when the equation is written in Cartesian co-ordinate system. Gaussian beam is the lowest order Laguerre Gaussian beam. Orbital momentum for trapped particle can be transmitted with the help of these beams, causing the particle to revolve about optical axis. Laguerre Gaussian tweezers can entrap metallic particles or particles with a refractive index greater the surrounding medium. Laguerre Gaussian tweezer is referred to as ‘optical vortices’.

Bessel Beams

The complex amplitude of Bessel beam is an accurate solution of Helmholtz equation opposite to a Gaussian beam whose envelope is the approximate solution of same equation. The distribution of intensity of Bessel beam is proportional to a Bessel function which is oscillatory in nature and is slowly decaying whereas Gaussian beam decays exponentially. Bessel beam have planar wave front with non-uniform intensity

distribution. These work in non-diffracting modes, due to their property of self-reconstructing after confronting an obstacle.

Its application is in concurrent trapping of several particles over long axial distances and it is possible by the use of only one single Bessel beam. The production of Bessel beams needs some particular schemes.

Gaussian Schell Model Beams

The transmission of partially coherent Gaussian beam can be explained in homogeneous medium by several methods and one of them is Gaussian Schell model beam. Gaussian Schell model beams can be created by superimposition of independent coherent Gaussian beams.

These beams are non-uniformly partially polarized. The partial coherence of these beams have an advantage of reduced ringing effect which is very common in complete coherent sources and also high directionality is evident due to this property of partial coherence.

Cylindrical Vector Beams

Conventional polarization states for example linear, circular and elliptical polarization can be explained by point on the Poincare sphere; the spatial inhomogeneous polarization state is possessed by vector beams and henceforth cannot be explained by a single point in spite of this they are explained by multiple numbers of points on Poincare sphere. By changing phase retardation or the orientation of wave plate, complete area of Poincare sphere can be covered. Polarization of a cylindrical vector beam is axially symmetric to the optical axis. A spatial light modulator is used to flexibly generate cylindrical vector beams. These beams are essential in analysis of particle orientation functions, microscopic applications and in atomic systems where different polarizations explain different selection rules.

Hollow Gaussian Beam

These beams are representation to define dark hollow beams. The area of dark region around Hollow Gaussian beam (HGB) can be restricted by using appropriate beam parameters. These can be generated by Fourier transforms of differential of Gaussian beam. Hollow Gaussian beams can be produced by arranging resonator having diffraction optical elements. The optical intensity of HGB may be altered by changing polarization angle and order of HGB. It can be represented as superimposition of series of Laguerre Gaussian modes.

Flat Topped Gaussian Beam

Flat topped Gaussian field is achieved by superimposing several Gaussian beams of diverse sizes. We can raise the slanting trapping range of planes close to the focal plane by enhancing the flatness of flat-topped beam and boost the longitudinal and transverse entrapping range at focal plane by reducing initial coherence of flat topped beam. The entrapping rigidity of flat topped beam decreases as beam order is increased or initial coherence is decreased.

Lorentz Beam

The type of transverse pattern in source plane of these beams is obtained to be the multiplication of two non dependent Lorentz functions. This is appropriate for describing certain laser sources for example in Double Hetro-junction Lasers. The M^2 factor of Lorentz beam does not depend on beam parameters; it is constant value equivalent to $\sqrt{2}$. M^2 factor directly indicates the divergence of beam and hence divergence of this beam is $\sqrt{2}$ (1.414) times that of Gaussian beam whose beam propagation factor is equivalent to 1.

Lorentz Gauss Beam (LGB)

Lorentz Gauss beam (LGB) has been proposed by Gawhary and Severini [2]. These are three dimensional scalar optical beams. They are called so because the shape of their transverse pattern in source plane is the multiplication of two non dependent Lorentz functions. LGBs are obtained by multiplying Lorentz beam function with the Gaussian function. The angular spread of Lorentz Gauss distribution is higher than that of Gaussian distribution. Therefore LGBs present model to depict radiation transmitted by any single mode diode laser. Lorentz beam is a distinctive case of LGB. It is a close explanation of paraxial wave equation. When w_{0y} and w_{0x} tend to infinity, the LGB converts to a Gaussian beam.

The M^2 factor of Lorentz Gauss beam is between 1 and $\sqrt{2}$. As the M^2 factor should be as near to one as possible, LGBs are better approximation for highly divergent beams [3]. For analysis of LGB in turbulent atmosphere the complete Huygens Fresnel integral and expansion of Lorentz function is used. The spreading of LGB is more rapid in turbulent atmosphere for large structure constant and small beam parameters [4].

1.6 Motivation and Goal of Work

All fundamental concepts connected with real Gaussian beams and real stable resonators were there in place by middle 1960s, as recognized in Kogelnik and Li's review [5] and in revised (1965) publication of Ramo, Whinnery and Van's text [6]. Real ABCD matrices, previously given in standard optical texts [7], are enforced to optical resonators [8, 9-13], they are transformed to now-a-days standard ABCD format [14, 15-17]. Kogelnik [15] identified bilinear conversion of q parameters (complex) over paraxial optical system incorporating the ray matrix. Chronological link between the degree of difference in the Gouy phase shift and phase shift of Gaussian mode [18, 19] was discovered; and Baues [20, 21] and Collins [22] prepared the peculiar examination that Huygens' integral over cascaded progression of paraxial optical elements can be written as particular integral containing the cascaded ray matrix of the system. The ultimate quarter of the last century has witnessed development of new concepts in optical resonators which encompasses paraxial beam propagation. The methodological advancements still persist that open new avenues today. These developments have been inspired by some new kinds of lasers, by demands for much more complex and multi element laser resonators, by developments in the laser beam propagation for possible applications, and by an enthusiasm for enhanced elemental knowledge of the optical beams and resonators.

The motivation behind this work is to analyze the beam properties of optical beams. Since Lorentz-Gauss beam is closest to Gaussian beam therefore it is chosen as one beam and Hermite-Gaussian beam is chosen because it is generalized beam. The goal of our work is to compare the two beams and find out the similarities and dissimilarities which will be helpful in the corresponding applications. Our goal is to compare two most essential beam properties of the two beams for the case of unstable resonator as it is used for high power Laser.

1.7 Outline of Dissertation

The following are the main objectives of this Dissertation:

1. To analyze the transmission of partially coherent LGB through a real and paraxial ray matrix system for the case of unstable resonator.
2. To analyze the transmission of partially coherent HGB through a real and paraxial ray matrix system for the case of unstable resonator.

3. To compare the beam properties of LGBs and HGBs during the propagation through a real and paraxial ray matrix system for unstable resonator.

The Dissertation is divided in 5 Chapters

Chapter 2 describes Properties of Optics i.e. types of coherence viz. Spatial and Temporal, degree of coherence; Matrix optics and Optical Resonators.

Chapter 3 gives Literature survey related to our work.

Chapter 4 describes Beam properties of LGBs and HGBs through real and paraxial ray matrix system for the case of unstable resonator.

Chapter 5 describes Conclusion and Future Scope of our work.

CHAPTER 2

Properties of Optics and Optical Resonators

2.1 Coherence

One of the essential concept of optics is coherence and the capability of light to display interference effects is directly related to this property of optics. Whenever a fixed phase relation is present between the values of electric field at distinct locations or at distinct times than the light field is said to be coherent. Partial coherence implies that there is imperfect correlation between different phase instances. Commonly the processes are called as coherent or in-coherent where coherent implies that the process is phase sensitive.

2.1.1 Degree of Coherence

A sequence of interference experiments is performed to measure the degree of coherence. EM theory is very important in coherence because of the polarization properties. It is also useful in material such as micro structured components [23-28]. According to the revised definition for the degree of coherence it remains constant if the field is revolved by using an appropriate anisotropic material. In EM wave the degree of coherence perform as invariant with the revolution of coordinate axes. For measuring far field coherence of EM waves the property of EM waves being constant in transformation in coordinate system is suitable [29].

The degree of coherence can be quantified by various ways they are described below.

- The degree of correlation is specified by correlation functions i.e. function of either spatial or temporal distance. The correlation functions are defined with the help of distinct orders. Optical spectrum is the first order correlation function. The effects like photon anti bunching or bunching are the phenomenon associated with intensity correlations and it is defined by the second order correlation function. Higher order functions gives more exquisite details.
- The measure of first order temporal coherence is quantified by the coherence time over the time through which quality of remainiing logical is lost.
- The coherence time times vacuum velocity of light is characterized by the coherence length, and it also defines the temporal coherence (but do not define spatial

coherence) through the transmission length and hence transmission time through which consistency is lost.

- Value of temporal coherence of single frequency laser is associated to the linewidth; a slender linewidth means elevated monochromaticity and it implies that temporal coherence is high.
- Fringe visibility parameters specifies the superimposition of two electric fields. It is generated by the pattern of visibility of interference.

2.1.2 Spatial Coherence

The spatial coherence is responsible for the relationship between waves and their point wise location in the space and consequently various electric fields are strongly related to one another in space when the spatial coherence is studied in a beam profile.

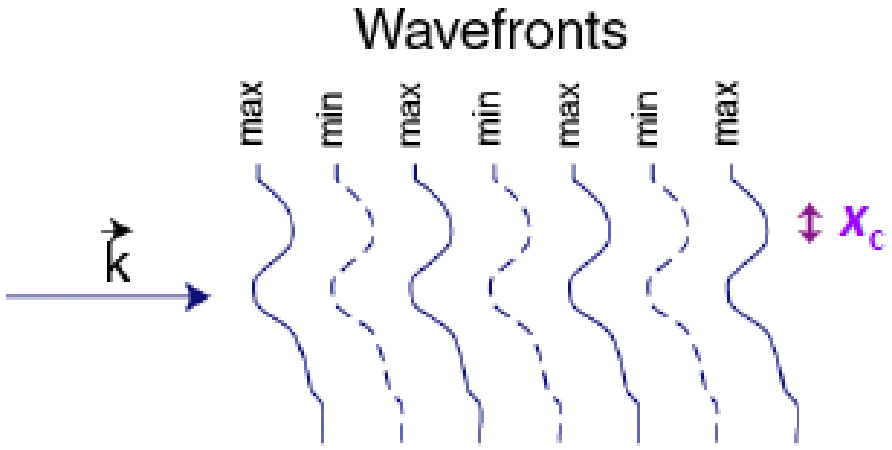

Figure 2.1 Spatial Coherence [30].

Figure 2.1 shows the Spatial Coherence with value of Spatial Coherence Length, x_c.

Laser result in producing beams which are spatially coherent in nature with a very high degree of coherence. This makes laser light different for application as compared to other ordinary light sources. For the strong directionality of Laser beams the Spatial coherence is most important prerequisite.

2.1.3 Temporal Coherence

Substantial correlation among electric field for one interval and different number of times is defined as Temporal coherence. As an illustration the output of a single frequency laser might be considered as it displays a very high temporal coherence, due to the clear sinusoidal oscillation exhibited by the field which briefly emerges in an extremely conventional fashion over complete period of time.

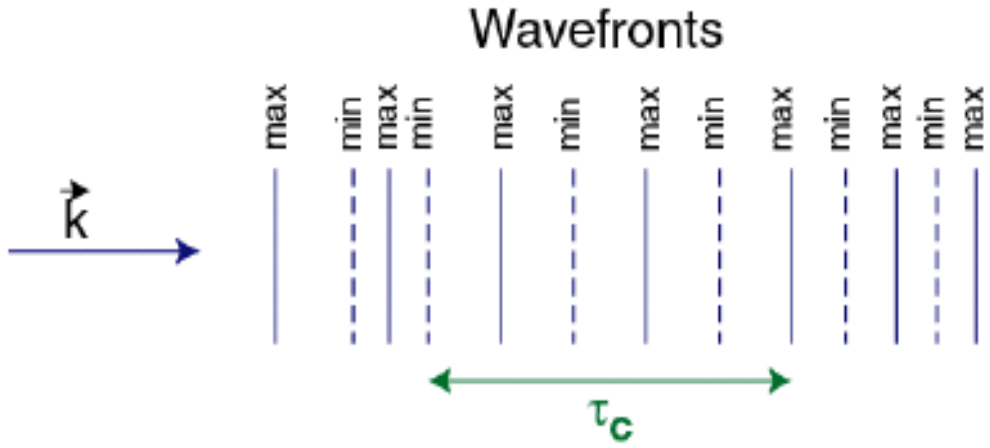

Figure 2.2 Temporal Coherence [30].

Figure 2.2 shows the Temporal Coherence with value of Temporal Coherence Length, c τ_c

2.1.4 Spatial and Temporal Coherence: Diagrammatical Illustration

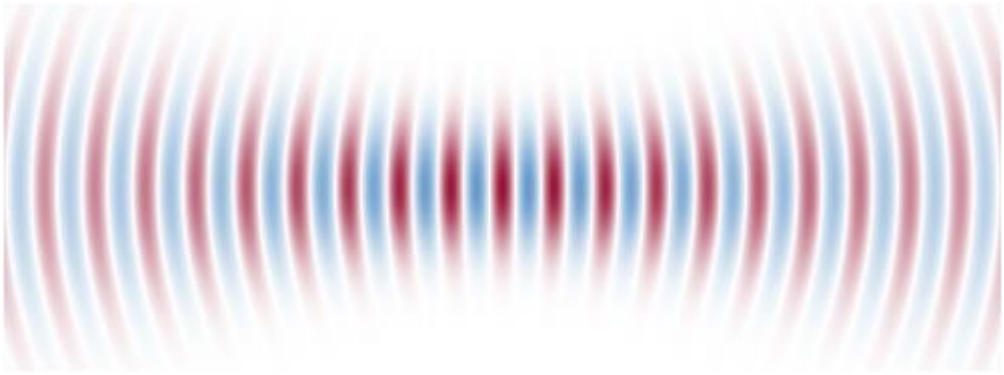

Figure 2.3 Gaussian beam presenting perfect spatial and temporal coherence [31].

Figure 2.3 presents a perfect spatial and temporal coherence exhibited by a monochromatic Gaussian beam. Gaussian beam is considered as ideal beam and properties of all other beams are compared with this beam. Therefore, here property of spatial and temporal coherence is given for Gaussian beam.

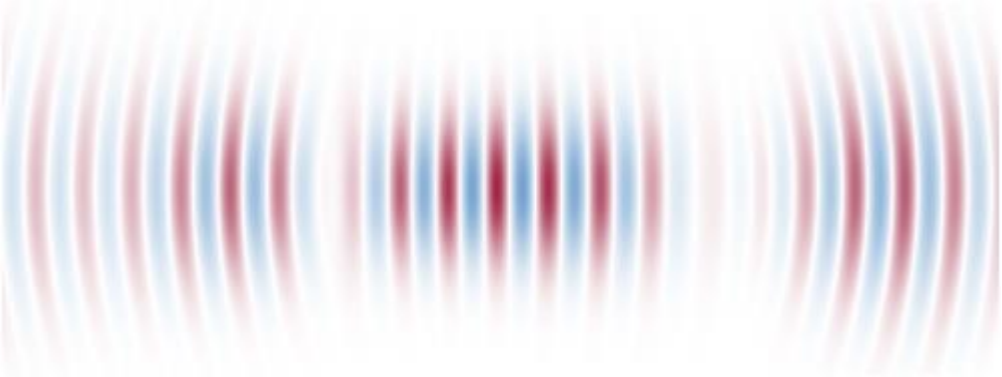

Figure 2.4 Optical beam representing poor temporal coherence and high spatial coherence [31].

Figure 2.4 represents a beam having poor temporal coherence and high spatial coherence. The wavefronts are created as shown in above figure, the phase and amplitude of beam alters along the transmission direction and beam quality is still high. In this case both the spacing and the local amplitude of wave fronts differ to some amount. This type of beam is usually obtained from the output of a source which is supercontinuum in nature.

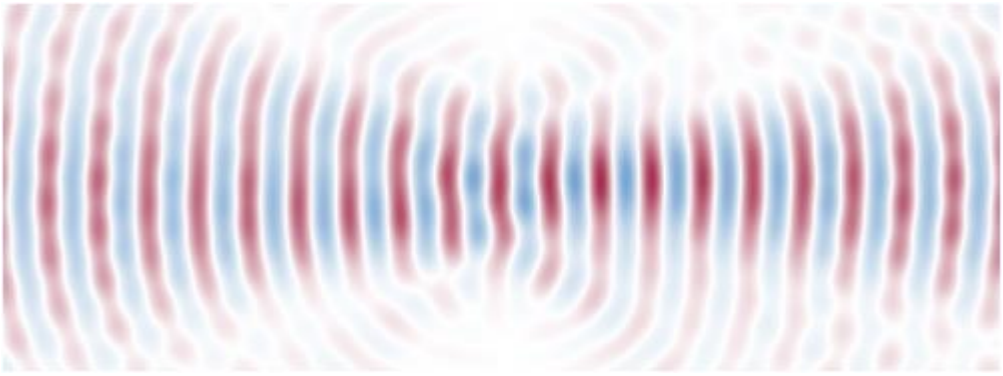

Figure 2.5 Optical beam representing high temporal coherence and poor spatial coherence [31].

Figure 2.5 represents a beam having high Temporal coherence and poor Spatial coherence. Due to poor Spatial coherence the wave fronts are distorted, resulting in a poor beam quality and high divergence. On the other hand due to high Temporal coherence, the beam is monochromatic, resulting in constant spacing of the deformed wavefronts. When the output of a single frequency laser is passed through inhomogeneous optical material than this type of beam is obtained.

- **Representation of Spatial and Temporal coherence**:

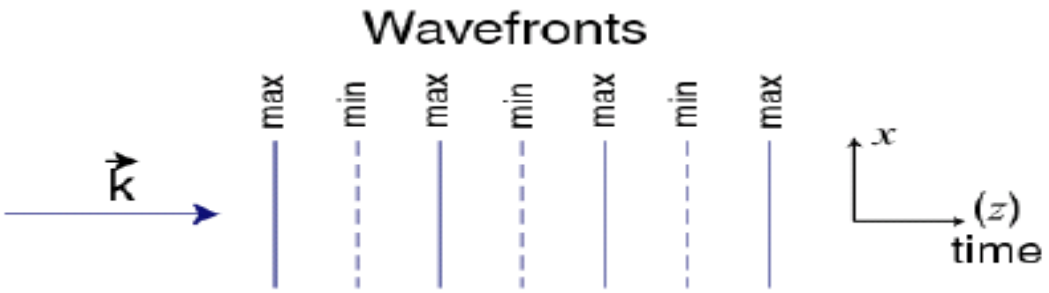

Figure 2.6 Spatial and Temporal Coherence [31].

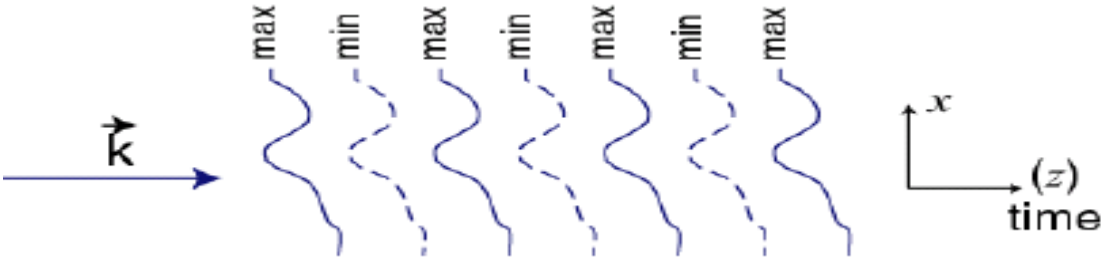

Figure 2.7 Temporal Coherence; Spatial Incoherence [31].

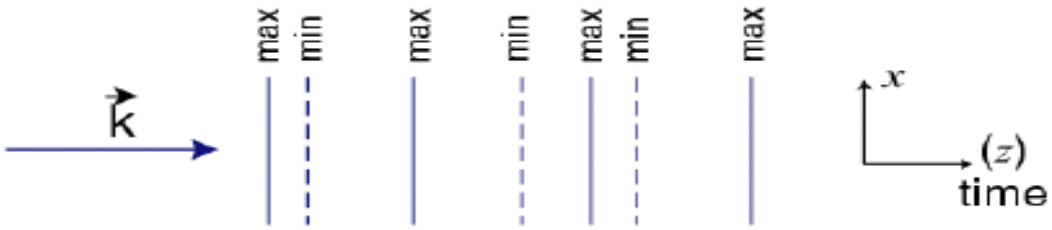

Figure 2.8 Spatial Coherence; Temporal Incoherence [31].

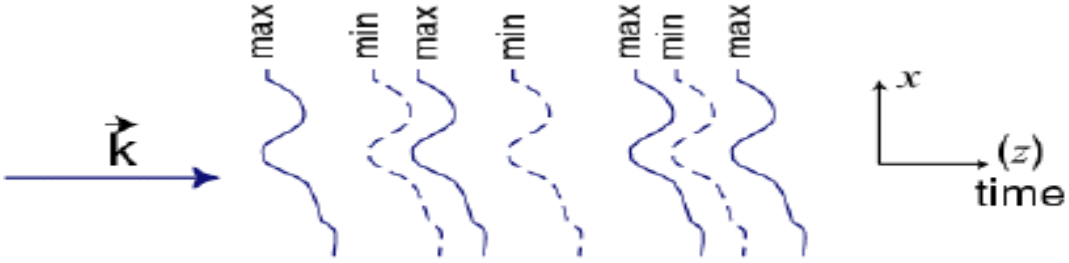

Figure 2.9 Spatial and Temporal Incoherence [31].

In the above figures from 2.6 to 2.9 Different types of Spatial Coherence or Incoherence; Temporal Coherence or Incoherence is shown.

2.1.5 Importance of Coherence in Applications

- Coherence with reference to phase and time gives rise to various applications and this is the reason that very high degree of spatial and temporal coherence is needed. The resonator mode creates spatial coherence of desired need. The two coherences viz. spatial and temporal coherences find application in fiber-optic sensors, holography and interferometry.
- It is used in coherent beam combining.
- The coherence of light should be small for other applications. For instance, very low Temporal coherence along with high Spatial coherence is needed for coherence tomography, here a kind of interferometry is used to create images, and large spatial resolution depends upon small temporal coherence. For such applications befitting light sources can be established on super continuum generation in nonlinear media or on ASE (amplified spontaneous emission) against laser amplifier (super luminescent source).
- A low degree of temporal coherence decreases the problem of speckle and similar interference effects so it can be helpful for imaging, pointer applications and laser projection displays.

2.2 Matrix Optics

To trace Paraxial waves we use the Matrix optics technique. It is assumed that rays are travelling within a single plane so that formualism remains planar and meridional for spherical rays.

To describe a ray two specifications, ray's position and angle are needed corresponding the optical axis. The above mentioned values changes with the propagation of ray in the system. In the paraxial approximation, there are two linear algebraic equations which relate the angle and position of ray at input plane and output plane of the given optical system. Due to this relation we need a 2×2 matrix to describe the optical system. This matrix is called as ABCD i.e. Ray transfer matrix.

Advantage of use of ray optics is when we have to calculate a Ray transfer for a complex system which is cascaded form of several optical systems; the output can be calculated by taking product of individual optical system [32].

2.2.1 The Ray-Transfer Matrix

Consider a circularly symmetric system which is created by a series of reflecting and refracting surface with all of them focused around the same optical axis. Z-axis points in direction of transmission, it lies along the optical axis.

Consider y-z plane contains the optical axis and hence rays are in this plane. A ray is traced as it travels through the system or in other words the path of the ray is traced when it passes transverse planes at distinct axial distances.

The traversal of ray is defined by y coordinate of its crossing point and θ angle. An optical system is defined as a set of optical components which are placed between two transverse planes at z_1 and z_2. They are introduced as input plane and output plane respectively as shown in figure 2.10.

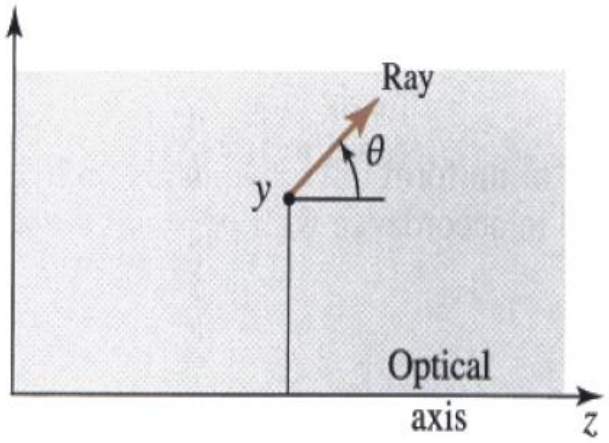

Figure 2.10 A Ray Characterised by its coordinate y and angle θ [32].

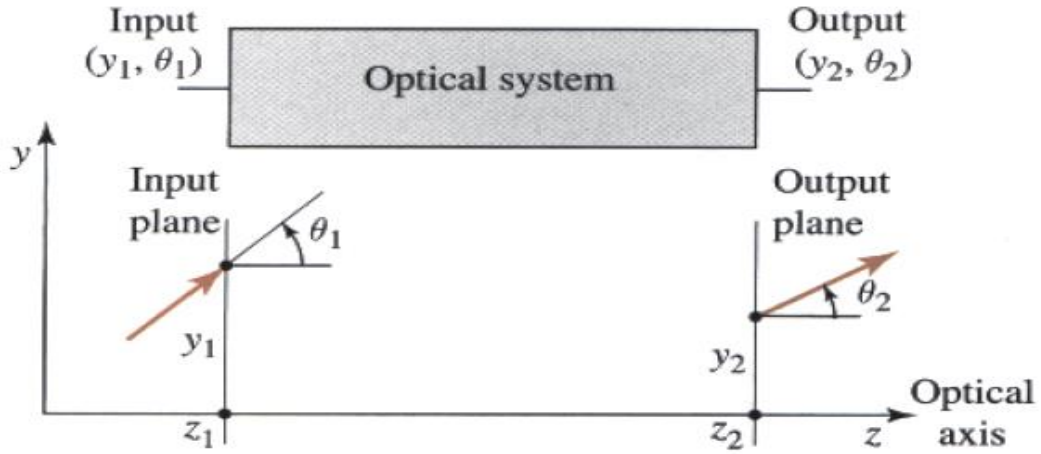

Figure 2.11 A ray entering the system at location z_1 with y_1 and θ_1 and leaves at location z_2 with y_2 and θ_2 [32].

In the paraxial estimation theory, if all the angles are so small such that we can consider, $\sin\theta \approx \theta$, than the relationship between (y_2, θ_2) and (y_1, θ_1) is linear and can be written as:

$$y_2 = Ay_1 + B\theta_1 \quad (2.1)$$

$$\theta_2 = Cy_1 + D\theta_1 , \quad (2.2)$$

Where *A*, *B*, *C*, and *D* are real valued integers.

Now, Equations (2.1) and (2.2) can be defined in matrix form as follows,

$$\begin{bmatrix} y_2 \\ \theta_2 \end{bmatrix} = \begin{bmatrix} A & B \\ C & D \end{bmatrix} \begin{bmatrix} y_1 \\ \theta_1 \end{bmatrix}, \quad (2.3)$$

The matrix M completely defines the system with components *A*, *B*, *C*, and *D* because this matrix allows that (y_2, θ_2) can be calculated for any (y_1, θ_1) .

2.2.2 Matrices of Simple Optical Components

Table 1

S.No	Optical System	Ray Transfer Matrix
1.	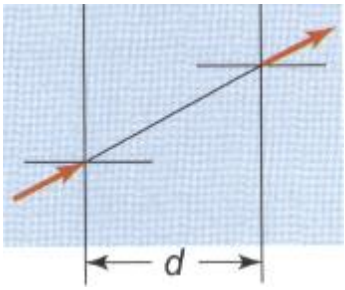	$M = \begin{bmatrix} 1 & d \\ 0 & 1 \end{bmatrix}$
2.	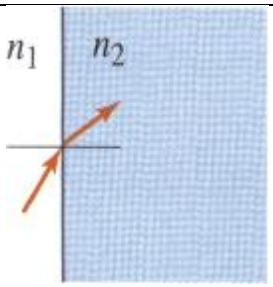	$M = \begin{bmatrix} 1 & 0 \\ 0 & \frac{n_1}{n_2} \end{bmatrix}$
3.	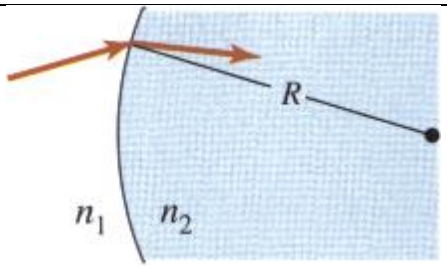	$M = \begin{bmatrix} 1 & 0 \\ -\frac{(n_2-n_1)}{n_2 R} & \frac{n_1}{n_2} \end{bmatrix}$

4.	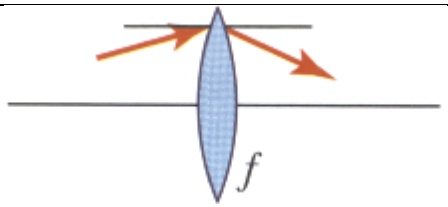	$M = \begin{bmatrix} 1 & 0 \\ \frac{-1}{f} & 1 \end{bmatrix}$
5.	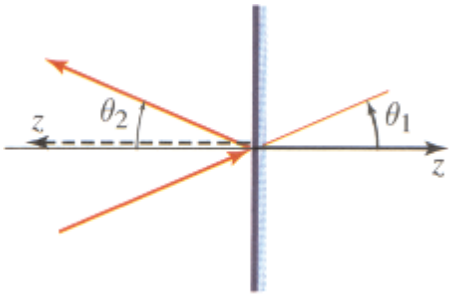	$M = \begin{bmatrix} 1 & 0 \\ 0 & 1 \end{bmatrix}$
6.	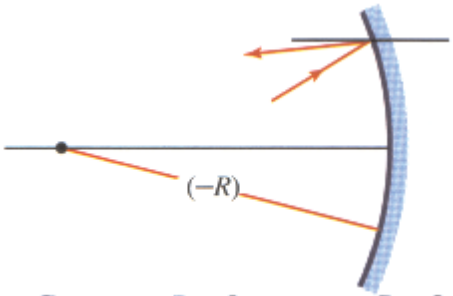 Concave: $R < 0$; convex: $R > 0$	$M = \begin{bmatrix} 1 & 0 \\ \frac{2}{R} & 1 \end{bmatrix}$

In table 1, Ray matrix of six elementary optical systems is shown. These are described below:

- Ray matrix No. 1 describes Free space propagation with $y_2 = y_1 + \theta_d$ and $\theta_2 = \theta_1$.
- In Ray matrix No. 2 Refraction at a planar boundary is shown. According to Snell's law for paraxial approximation $n_2\theta_2 = n_1\theta_1$ and $y_2 = y_1$.
- Ray matrix No. 3 is the case of Refraction at a spherical boundary, here the height of the ray remains unaltered i.e., $y_2 = y_1$ and $\theta_2 = \frac{n_1}{n_2}\theta_1 - \frac{n_2 - n_1}{n_2}\frac{y}{R}$.
- Transmission through a thin lens is defined by Ray matrix No. 4 with height $y_2 = y_1$ and $\theta_2 = \theta_1 - \frac{y}{f}$.

- Ray matrix No. 5 shows Reflection from a planar mirror where the height remains $y_2 = y_1$ and $\theta_2 = \theta_1$.
- In Ray matrix No. 6 Reflection from a spherical mirror is shown it is identical to the transmission through a thin lens whose focal length is given as $-R/2$, where R is radius of curvature.

2.3 Optical Resonator

Resonator is adjustment of optical components which permit a beam of light to distribute in a closed path. A resonator with given properties can be designed by using technically interesting methods which are often of numerical nature. The alignment sensitivity and the beam quality are some of the various aspects of laser operation which are influenced by the design of a laser resonator.

Application of Optical Resonators:

- The resonator losses are reimbursed by a gain medium to retain the optical power using laser resonators.
- They are used as etalons for windowing the frequency contented by the optical radiation.
- Mode cleaner cavities are used for filtering the transverse form of optical radiation.
- When the frequency of a laser is linked to a resonance frequency of stable reference cavity the optical resonator is used as short term optical frequency standard.
- When the resonator length is changed the periodically occurring resonances are exploited by using optical resonator for precise length measurements.
- Enhancement cavities are used for exploiting the resonant enhancement of intra-cavity power, in order to attain efficient frequency duplication of light from single frequency low power laser.
- The decay of the power of intra-cavity radiation is recorded by using cavity ring down spectroscopy for precisely measuring low level losses.
- With a Gires–Tournois interferometer chromatic dispersion effects are generated.

2.3.1 Stable Resonator

Most solid state bulk lasers are established on the concept of stable resonators. The properties and adjustment of the optical components, primarily the curvature of reflecting surfaces, the distances between the components, and other focusing effects are the factors on which stability of a resonator depends. The resonator may go through different stability zones when a parameter varies; for instance when a parameter like dioptric power or an arm length of focusing element in the resonator is altered the resonator undergo different stability zones given as; one stability zone for ring resonators and two stability zones for standing wave resonators [34].

2.3.2 Unstable Resonator

The unstable resonator does not imply that it is less robust as compared to stable one. On the contrary, comparatively robust high power lasers have been grown with unstable resonators because the alignment subtlety of unstable laser resonators can be even considerably lower than for stable resonators.

Advantages of Unstable Laser Resonators

Although most laser resonators are constructed as stable resonators, there is a significant advantage of unstable resonator in certain cases. For such resonators the mode volume in the cavity might be large, which points to low power densities at the mirrors.

A laser beam with immense optical power and still comparatively high beam quality can be developed using unstable resonator. If stable resonator is used in such cases than a problem arises that is a big enough fundamental resonator mode cannot be accomplished, since this mode is extremely perceptive to disturbances like misalignment or thermal lensing. For such cases an unstable resonator is most appropriate because it can have a fundamental mode with a considerable net gain advantage over all other higher order modes, and with no superfluous sensitivity.

Limitations of Unstable Laser Resonators

A laser beam with immense optical power and still comparatively high beam quality can be developed using unstable resonator but this principle is usually valid only when the gain medium can provide comparatively large gain.

The unstable resonator can only be used in high gain lasers for instance in pulsed diode pumped YAG lasers, flash lamp pumped, excimer lasers, metal vapor lasers, and chemical lasers. The application of unstable resonator to low gain lasers for example

continuous wave lamp pumped solid state lasers or CO lasers is comparatively more difficult and generally leads to a poor beam quality.

Henceforth, we need a gain medium with larger gain to obtain high optical power and high gain Laser beam.

2.3.3 Periodic Structure of Laser Cavity

In the Cavity the back and forth bouncing of an optical ray can be "unfolded" along the z axis. In other words, the light trajectory can be considered as a series of one-way paths from M_1 to M_2 then from M_2 to M_1 etc. To do that, we need to change the mirrors with radii of curvature R_i by lenses with focal lengths $f_i = {R_i}/{2}$.

Hence we find the structure equivalent to two-mirrors linear cavity which is a periodic structure formed by a series of lenses separated by a distance d. This structure is shown in figure 2.12.

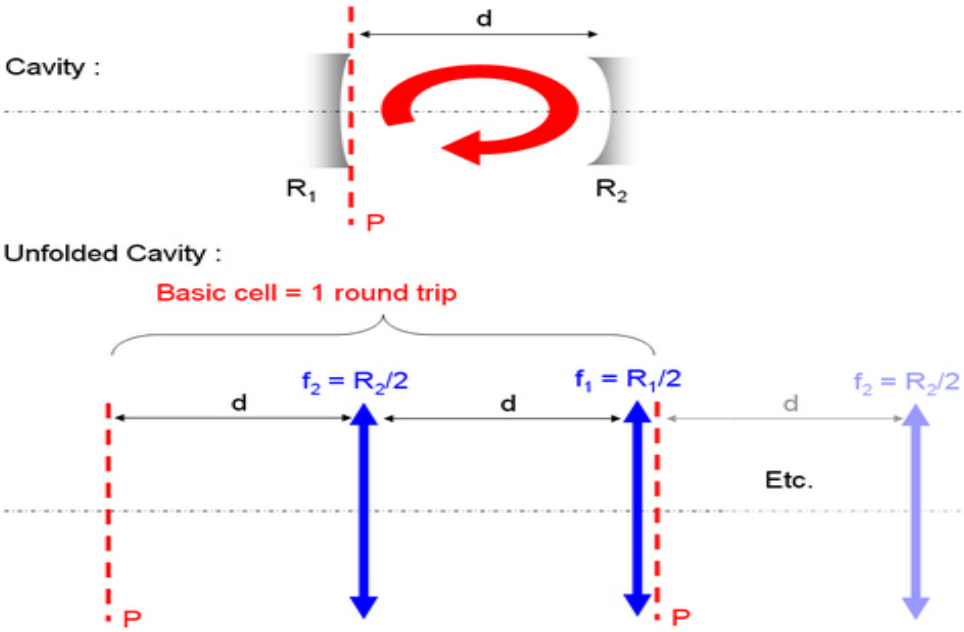

Figure 2.12 Unfolded Cavity [35]

If the rays remain in the proximity of the optical axis even after passing through the series of lenses than the cavity is considered to be stable; if it is not the case, than the cavity will be unstable.

CHAPTER 3

Literature Review

A new type of three dimensional scalar optical beam is given by Gawhary and Severini [2]. The shape of transverse pattern of these beams in source plane is multiplication of non-dependent Lorentz functions therefore these beams are called as Lorentz beams. A derivation for free space transmission in the paraxial limit is done and closed form expressions are obtained. The scalar paraxial wave equation is fulfilled by gradually varying component of the concerned field therefore it is clear that there exist Lorentz Gauss beam (LGB), these are beams found out by multiplication of the actual Lorentz beam with a function called as Gaussian apodization function. Even though presence of LGBs can be presented by using distinct and separate approaches given by Kiselev and Gutierrez Vega and Bandres here a third different approach is followed, which uses group theory given by Lie.

G. Zhou [3] investigated the M^2 factor of LGB based on second order moment. With the help of theorem of Fourier transform namely product theorem, the analytical formulae for M^2 factor are analyzed. The M^2 factors are independent from each other in the *x*- and *y*-direction. In this paper the value of M^2 factor of LGB is derived. Its value lies between 1 and 1.414. The value of M^2 factor of Gaussian beam is 1 and for Lorentz beam the value is 1.414. Hence, the LGB is a better approximation to describe some laser sources which produce immensely divergent beams.

X. Chu et. al. [4] presented that for analysis in turbulent atmosphere the extended Huygens Fresnel integral and expended Lorentz distribution is used. The spreading of LGB is faster in turbulent ambience for larger values of structure constant and small beam parameters. Uniaxial crystal contributes efficient yet favourable technique for modulation of LGB where a light beam with unique shape and polarization is required.

J. Tervo et. al. [29] showed that the traditional description of degree of coherence of EM field is improper and a novel quantity is introduced which do not possess the prescribed flaws. The presented description is proved to be true with acknowledged results for statistics of Gaussian function, and it has several exceptional characteristics which are the

peculiar characteristics of EM fields only. Degree of coherence can be assessed by a arrangement of experiments of interference. The relation between fringe visibility and spatial degree of coherence in EM wave is described by two pinhole interference method.

Naqwi A and Durst F. [36] presented that Lorentz-Gaussian distribution occupies larger angular spread as analyzed with Gaussian distribution; and hence it presents further more accurate representation to characterize the emission transmitted from single mode laser. For simple and rather accurate calculations of optical field in focal region an interpreted statistical model for far field of mono mode laser is represented. The treatment given in this paper is connected with junctions of laser which are much limited than the wavelength. Detailed discussion of the field distribution on plane orthogonal to junction of diode is done. Hence, for designing of optical devices, for instance laser Doppler anemometers and diode fiber couplings the described mathematical code is of significant importance. The work presented is not involved with propose calculations for definite functions. Instead, the intention of this paper is to exemplify the familiar sort of proposed precise model of mono mode laser beams.

Dumke W P. [37] presented that LGB is also applicable to describe a range of double hetero-junction $Ga_{1-x}Al_xAs$ lasers which are available in market, active region of these lasers are as contracted as 0.1 μm for a radiating wavelength of 0.8 μm. Hence, LGB presents a more suitable model to explain non-paraxial laser. In past years, the transmission of several laser beams is given by solution of Maxwell's equations in uniaxial crystals, in case of beam propagating perpendicular to and along the optical axis.

Jia Li et.al. [38] presented that Anisotropic media is playing an important role in designing polarizers and compensators. Properties of diffraction of LGB when analysed in media which is anisotropic in nature gives the result as, on transmission in uniaxial crystals, the symmetric distribution of LGB is lost and their respective speed of spreading is different in x and y directions, it is due to the effect of media used. When the LGB radiates in far field, the distribution of intensity profile will change into a profile having four petals by preferring a distinct width of beam waist for Lorentz part in plane, distributions of intensity would differ upon propagation.

G. Zhou [40] presented that to accurately propose optical system that involves single mode laser, study of transmission of LGB traversing through ray matrix system is to be done. Laser beams are roughly partially coherent in feasible systems [39], it describes that entirely coherent laser sources are not possible practically. Ray matrix is used to explain random optical system in optics.

By developing the erfc (complementary error function), M^2 factor of partially coherent LGB is proved to be higher than the relative Gaussian beam. With increase in spatial coherence length, LGB has narrower effective beam size and larger complex spatial degree of coherence.

Yunfeng Jiang et. al. [41] presented that LGB can be used to entrap the molecules whose refractive index is higher than that of atmosphere. There are a lot of applications of optical trapping to manipulate particles. Usually Gaussian beams were used for the purpose of optical trapping but afterwards many other beams came out to be valuable for this purpose. Emission forces fashioned by laser are mostly associated to the characteristics of beam for instance polarization and beam shape.

Xun Wang et. al. [42] presented the numerical characteristics of non paraxial LGB are calculated by preliminary parameters of beam and parameters of crystal. Conclusions show that even with y component of LGB in input plane as zero, y and longitudinal components will arise upon transmission in uniaxial crystal, which must not be mistreated. This is because of the change of polarization state of the radiation which takes place while beam is propagating in uniaxial crystal [43].

The sizes of beam waist not only have an effect on both shape, size of profile of beam in uniaxial crystal but additionally it finds out the nonparaxial effect of LGB; even with only one of the three parameters being analogous with wavelength of light, the beam must be considered outside the paraxial estimation.

Generally, the Lorentz-Gauss beam is designed by double hetero junction $Ga_{1-x}Al_xAs$ laser resonator; therefore it will have immense divergence in far field [36]. Lorentz Gauss beams are analyzed in turbulent atmosphere due to the utilizations in remote sensing and optical communications in free space. Due to influence of anisotropic medium on crystal, profile of beam is expanded in x direction, although w_{0x} is equal to w_{0y}. Consequently, the shape of beam profile is associated to w_{0x} and w_{0y} and the amount of spot increase with $w_{0.}$

A. Keshavarz and G. Honarasa [44] demonstrated that the distribution of intensity and beam width of LGB diverge at regular intervals during transmission. In this paper, the intensity distribution, beam width and radius of curvature were calculated using ABCD method and Collin's formula.

G. Zhou [45] presented the Kurtosis parameters for Lorentz Gauss beams. In this paper it was shown that kurtosis parameter of LGB via real ray matrix system depends on two components. Where one component is associated to the fraction of width of Lorentz part and waist of Gaussian part; another component is the proportion of matrix variable B to the multiplication of matrix variable A and without diffraction range of Lorentz part.

Hong yu et. al. [46] presented that in non paraxial system angular spread of LGB is generously proportioned than that of Lorentz beam having similar beam width. Propagation equations are derived using diffraction integral by Rayleigh Sommerfeld. In this paper, methodical propagation equations for non paraxial Lorentz; LGB in free space have been deduced and some appealing unique cases are discussed. The angular scattering depends on beam standards namely Lorentz, Lorentz Gauss and beam width. In non paraxial system the angular spread of Lorentz Gauss beam is bigger as compared to the angular spreading of Lorentz beam with identical beam width.

H. Laabs [47] compared the findings of expansion theory with electromagnetic propagation. The non paraxial conclusions of theory of expansion are correlated with theory of diffraction. Using the non paraxial alteration for Hermite Gaussian modes having intricate arguments unambiguous formulae for non paraxial alteration of standard Hermite Gaussian beams (SHGB) are obtained. The transverse alterations totally persuade the electromagnetic theory. The relevance of the result obtained in this paper is for the computation of extremely divergent eigen modes of resonators and also the results are useful for relating the transmission of extremely divergent beams.

Depending on the technique of truncated second-order moment, G. Zhou [48] derived the systematic expression of general beam propagation factor meant for reduced partially coherent Lorentz beam. The parameter for coherence 'τ' and parameter for truncation 'β' are used for calculating M^2 factor of reduced partially coherent Lorentz beams. An

approximate numerical expression of M^2 factor of reduced partially coherent LGB is specified with the help of complicated Gaussian expression of function for aperture of system. M^2 factor of reduced partially coherent LGB depends on the three parameters explicitly parameter for truncation 'β', parameter for coherence 'τ' and beam parameter 'a'. The formulae obtained in this paper are applicable for feeble truncation case and barely hold for strong truncation case; as for strong truncation case the beam truncation arises due to diffraction. The M^2 factor of reduced partially coherent Lorentz and LGBs are described by mathematical illustrations, and dependence of M^2 factor on different parameters is discussed by using the derived expressions. This research is useful for the realistic applications of reduced partially coherent Lorentz and LGBs.

In this paper G. Zhou [49] presented energy flux distributions of LGB, vectorial form of the LGB is revealed by showing the transverse electric and transverse magnetic terms in far field reference plane. The transverse electric and transverse magnetic terms of LGBs are revealed and dependency of different sets of parameters on distribution of flux energy of LGB is discussed. In addition to it, vectorial structure of LGB and Gaussian beam is also compared. For highly divergent beams LGB gives a far better suitable model to depict some laser sources as matched with Gaussian beam.

The M^2 factor is calculated by S. Saghafi and C.J.R. Sheppard [50] for higher order Gaussian beams, for rectangular coordinates they are comprising of two types: regular and elegant of Hermite–Gaussian functions, and for cylindrical coordinates also they are comprising of two types: regular and elegant of Laguerre–Gaussian functions. In general, the M^2 factor is minor for elegant modes, and it increases gradually with mode number.

In this paper Ji X and Li X [51] studied guidance of Gaussian arrays transmitting in turbulent atmosphere and the attribute of guided beam is given as angular spreading. Standardized far field typical distribution of intensity is analyzed and guidance of Gaussian arrays is calculated in expression of angular spread. Derivation for Close form expression of mean square of beam width and angular spreading of Gaussian beams transmitting in turbulent atmosphere are done. Here, it is observed that for example of coherent combining, in some conditions array of beams are there which might possess similar guidance it shows that the angular spread is same as that of a completely coherent

Gaussian laser beam in turbulence as well as in free space. In contrast to this, in terms of standardized far field average intensity allocation in free space, the guidance of Gaussian beams in expressions of angular spreading is inconsistent; whereas as a result of turbulence they may be consistent.

In this paper Eyyuboğlu HT [52] studied Hermite cosine Gaussian beams (HcosGB). Dependence of HcosGB on the source parameters is studied and its source plane intensity is proposed. With the application of diffraction integral given by Fresnel, the formulation is done for average intensity of HcosGB for receiver for transmission in atmospheric turbulence. In several unusual cases, the average intensity for receiver is observed to decrease appropriately. When propagating in turbulence, initially the merging of neighbouring beam lobes is experienced by HcosGB, then a transverse electromagnetic form cosh Gaussian beam is produced which leads to provisionally plain cosh Gaussian beam. Eventually is a pure Gaussian beam is obtained as a result. It is indicated by the mathematical estimation of standardized beam size along axis of propagation on certain mode indices so as to get the comparative spread for higher order HcosGB modes less than that of lower order analogue. As a result, by the use of higher mode HcosGB for some propagation distance it is probable to capture some more power.

Hyo-Chang Kim and Yeon H. Lee [53] derived the accurate electric field vectors of superior order Laguerre Gaussian and HGB by using the electric field divergence theorem and angular spectrum method on the slanting components of electric field given at z=0 plane. It is proved that the overall beam power is preserved alongside the beam propagation direction. By the use of Lommel's lemma power-series solutions are calculated from exact solutions. These solutions are shown to be exactly satisfying Lax's equations.

In the circumstance that the fading waves are ignored; Qing Cao and Ximing Deng [55] derived a comparatively straightforward transform from a random solution of paraxial wave equation to the equivalent exact explanation of Helmholtz wave equation. It is used to analyze alterations of paraxial estimation of random free propagation beam. Some particular examples are presented, such as smallest order alteration to paraxial estimation of elementary Gaussian beam. The waist plane has parallel shift from z = 0 plane.

Guoquan Zhou [56] derived a numerical result for LGB determined by an optical system having thin lens and aperture is circular, depending upon diffraction integral formula given by Collins and complicated Gaussian expansion of function of aperture. The dependency of focal shift on different parameters of focused reduced LGB is investigated and focal shift of focused reduced LGB is studied by the help of mathematical examples. The presented work is beneficial for the application of extremely divergent lasers.

Guoquan Zhou [57] applied fractional Fourier transform (FRFT) to the transmission of LGBs. Some laser sources which produce extremely divergent beams are studied using Lorentz–Gauss beams. A mathematical expression for LGB traversing through FRFT system has been derived depending upon description of convolution and convolution theorem of Fourier transform.

G. P. Agrawal and D. N. Pattanayak [58] studied the transmission of Gaussian beam in a local, homogeneous, nonmagnetic, linear and isotropic medium having dielectric material, using angular range illustration of electric field. Electric field inside the dielectric medium which is associated with the Gaussian beam consists of higher order non Gaussian alteration terms and the paraxial result. It is evident from the results presented in this paper that the second order alteration term holds true when compared with an equation dependable on the work of Lax, Louisell, and McKnight.

Riccardo Pratesi and Laura Ronchi [59] presented a new explanation of paraxially comparative equation of wave in free space. This solution is of the type of Hermite Gaussian function, with the complex argument of the Hermite polynomial. Special cases of general solution presented here are the usual Gaussian beams where such argument is real and where it is complex but corresponding to that of Gaussian function. The application of these general beams for a complex graded index medium is studied.

On the basis of vectorial integral formulae of Rayleigh Sommerfeld, Guoquan Zhou [60] derived the numerical propagation equation for non paraxial LGB for the case of free space transmission. The scalar paraxial result and far-field equation are also presented as particular cases of general formulae. Using mathematical examples, nonparaxial propagation characteristics of LGB are studied in free space. The transmission of LGB outside the paraxial estimation can be analyzed using approach of this research work.

Guoquan Zhou [61] investigated the transmission of partially coherent hollow vortex Gaussian beam (HVGB) via paraxial ABCD optical system in the turbulent atmosphere. With the help of numerical methods, the mathematical equations for degree of polarization and average intensity of HVGB in turbulent atmosphere are calculated without using any approximations. The influences of the topological charge, beam parameters, structure constant of turbulent atmosphere, and transverse coherent length on transmission of HVGB in turbulent atmosphere are also discussed. The dark region progressively declines until it disappears entirely as the propagation distance in turbulent atmosphere increases.

Takashi Takenaka et. al. [62] obtained all higher order alterations for Laguerre Gaussian and HGBs unambiguously. It is investigated that the alterations for both beams are explained in same format. The transmission of beam of light outside the paraxial approximation can be dealt by superimposing the corrected beams; when the field allocation of beam of light is specified at a number of transverse planes.

L. W. Davis [63] presented a comparatively easy method for finding out the characteristics of paraxial beam of electromagnetic emission transmitting in vacuum. This method gives the identical result for the lower order component of transverse and longitudinal electric field of Gaussian beam as derived by Lax, Louisell, and McKnight using a more complex technique. The central idea applied is that plane polarization is seen in the vector potential field. Scalar wave equation is followed by the non declining component of vector potential.

Y. Yuan et. al. [64] investigated the transmission of elegant Hermite Gaussian beam (EHGB) in atmospheric turbulence. Depending upon extended Huygens Fresnel integral numerical formulae for average intensity and effective beam size of an EHGB are also derived in atmospheric turbulence. Therefore, for the ease of assessment the equivalent results for standard Hermite Gaussian beam (SHGB) are also derived for the case of atmospheric turbulence. The mathematical and comparative analysis is done for spreading and intensity characteristics of EHGB, SHGB in atmospheric turbulence. It is observed that transmission properties of EHGB and SHGB are dissimilar when compared with their properties in free space, the effect of turbulence is a lesser amount for higher order.

EHGB and SHGB. It is also shown that the spreading of SHGB is more rapid as compared to EHGB in atmospheric turbulence under the identical situations.

Jiong Yang et. al. [65] used a partially coherent Lorentz model to explain far field for single mode laser. The work is perturbed with junctions of lasers which are significantly slender than the wavelength. To transform diverging beam into a converging beam two lens system is kept in front of laser. The spectral density function in plane orthogonal to junction of diode is discussed and later on it is used to guess intensity of light on several beam cross section areas close to focus by using general Huygens diffraction integral.

Guoquan Zhou [66] presented transverse electric and transverse magnetic terms of Lorentz beam corresponding to technique of vectorial structure and constant phase of electromagnetic beam. The description of the Lorentz beam is triggered by Maxwell's equations. Transverse magnetic term is positioned at x axis and is comparatively accumulated in y direction, whereas the transverse electric term is positioned at y axis and is comparatively accumulated in x direction. In the far field reference plane vectorial composition of Lorentz beam is depicted by transverse electric term and the transverse magnetic term which defines distribution of intensity of light of the Lorentz beam. Transverse electric and transverse magnetic terms of Lorentz beam and its influences on the dissimilarity of transverse beam waists on distribution of intensity of light are also analyzed. Due to fairly minute effect of diffraction the beam spot of Lorentz beam comes out to be smaller than the beam spot of Gaussian beam in the far field; whereas the beam spot of Lorentz beam is larger than the beam spot of Gaussian beam at source plane. The effect of diffraction of Lorentz beam is weak for the paraxial case whereas for the non-paraxial case, it is obvious.

Chengliang Zhao and Yangjian Cai [67] derived the numerical propagation formulae depending on the general Huygens Fresnel integration for Lorentz and LGB which are partially coherent passing through paraxial ray matrix system in turbulent atmosphere. For instance, focusing quality of partially coherent Gaussian, LGB and Lorentz beam are analyzed in turbulent ambient; numerically and comparatively. The focusing properties of these beams in atmospheric turbulence are found to be clearly dissimilar from those in free space and these are calculated by structure constant and initial turbulence coherence. Partially coherent Lorentz beam could be focused more firmly than partially coherent

Gaussian or LGB in atmospheric turbulence with minute constant at geometrical focal plane or in free space. The benefit of Lorentz beam over Gaussian or LGB disperse progressively with declination in initial coherence or increase in structure constant.

In this paper B. Rose et.al. [68] demonstrated that for analyzing random optical systems; complex *ABCD*-matrix techniques together with Huygens Fresnel law are general wave optics tool. Several applications of practical interest in statistical optics have been studied. Particularly in all cases, close form numerical solutions are obtained. These solutions have direct physical interpretations and are useful for parametric systems studies.

CHAPTER 4

Beam Properties of Lorentz-Gauss and Hermite-Gaussian beams for Unstable Resonator through Paraxial ABCD Optical System

4.1 Introduction

The ultimate quarter of the last century has witnessed development of new concepts in optical resonators which encompasses paraxial beam propagation. The methodological advancements still persist that open new avenues today. These developments have been inspired by some new kinds of lasers, by demands for much more complex and multi element laser resonators, by developments in the laser beam propagation for possible applications, and by an enthusiasm for enhanced elemental knowledge of the optical beams and resonators.

In this work we have analyzed the beam properties of optical beams. Lorentz-Gauss and Elegant Hermite-Gaussian beams have been selected for this work. The M^2 factor of LGB is between 1 and $\sqrt{2}$. As the M^2 factor should be as near to one as possible, LGB are better approximation for highly divergent beams. Hermite-Gaussian beams (HGB) are the generalized form of optical beams which have wavefront similar to Gaussian beam. These types of beams can replicate between spherical mirrors that form resonator without getting distorted. They are self producing waves and therefore referred as resonator modes.

We investigated two important beam parameters of optical beams i.e. Effective beam size and Spatial complex degree of coherence. These two beams are compared on the basis of the above mentioned properties. For the practical application of a beam; the behaviour of beam while propagating in any optical system is examined using these parameters.

The two beams are found to be closely related as our results indicates that the Spatial complex degree of coherence is same for two beams. On the contrary, the behaviour of beams for Effective beam size is found to be opposite. Due to this phenomenon the two beams can be used for the applications according to the need of Effective beam size.

Our goal is to find the threshold point for the Effective beam size after which the response of beam changes abruptly. The coherence length plays very important role as for very small changes in the coherence length we are getting significantly large difference in the curves of Effective beam size.

ABCD matrix is convenient to use for this purpose because of the simplicity involved in complex optical systems. Here in this work we have used the Real *ABCD* matrix considering there is no aperture in the optical system involved. Therefore the values of parameters remain to be real, we can use complex values as well but for the ease of calculation and better understanding real matrix is chosen.

4.2 Methodology: Mathematical Analysis

To trace Paraxial waves we use the Matrix optics technique. It is assumed that rays are travelling within a single plane so that formualism remains planar and meridional for spherical rays. We need a 2×2 matrix to describe the optical system.

We solved the paraxial wave equations using Ray matrix which is convenient to use for complex optical systems as only cascading of ray matrices needs to be done to solve any complex optical system which turns out to be the product of matrices and is easy to calculate.

The condition for the stability of a resonator is given by trace of ABCD matrix [33]:

$$-1 \leq \frac{A+D}{2} \leq 1, \text{ or}$$

$$0 \leq \frac{A+D+2}{4} \leq 1$$

As we are studying the beams for unstable resonator therefore the values of ABCD parameters should be such that,

$$-1 \geq \frac{A+D}{2} \geq 1, \text{ or}$$

$$0 \geq \frac{A+D+2}{4} \geq 1$$

In this work, mathematical analysis is divided into two parts: 1) Calculations for Effective beam size and Spatial complex degree of coherence of Lorentz-Gauss beams and 2) Calculations for Effective beam size and Spatial complex degree of coherence of Hermite-Gaussian beams.

4.2.1 Lorentz-Gauss Beams:

Lorentz Gauss beams are described using Helmholtz equation. The propagation axis is assumed to be z-axis in Cartesian coordinate system. $\Gamma(x_{0a}, x_{0b}; y_{0a}, y_{0b}; 0)$ is characterized

as the function for mutual coherence of partially coherent LGB in the plane z=0 and is defined as,

$$\Gamma(x_{0a}, x_{0b}; y_{0a}, y_{0b}; 0) = \mathrm{E}(x_{0a}, y_{0a}, 0) \times \mathrm{E}(x_{0b}, y_{0b}, 0) \times \mathrm{g}(x_{0a}, x_{0b}; y_{0a}, y_{0b}; 0)\,, \quad (4.1)$$

Where $\mathrm{E}(x_{0a}, y_{0a}, 0)$, $\mathrm{E}(x_{0b}, y_{0b}, 0)$ and $\mathrm{g}(x_{0a}, x_{0b}; y_{0a}, y_{0b}; 0)$ are given as,

$$\mathrm{E}(x_{0s}, y_{0s}, 0) = \frac{1}{w_{0x} w_{0y} \left[1+\left(x_{0s}/w_{0x}\right)^2\right]\left[1+\left(y_{0s}/w_{0y}\right)^2\right]} \times \exp\left(-\frac{x_{0s}^2+y_{0s}^2}{w_0^2}\right), \quad (4.2)$$

$$\mathrm{g}(x_{0a}, x_{0b}; y_{0a}, y_{0b}; 0) = \exp\left[-\frac{(x_{0a}-x_{0b})^2}{2\sigma_x^2} - \frac{(y_{0a}-y_{0b})^2}{2\sigma_y^2}\right], \quad (4.3)$$

where s=1 or 2 , w_{0x} is beam width parameter of Lorentz part in x direction and w_{0y} is the beam width parameters of Lorentz part in y direction, beam waist for Gaussian part is defined as w_0. Schell-model source generates spatial complex degree of coherence of beams given as $\mathrm{g}(x_{0a}, x_{0b}; y_{0a}, y_{0b}; 0)$. The spatial coherence length is given as σ_{x} in x direction and σ_y in y direction. Exp(-$i\omega t$) is the factor depending on time and it is skipped in equation 1, here circular frequency is given as ω. Linear superimposition of Hermite-Gaussian functions is defined as the Lorentz distribution and is given as:

$$\frac{1}{(x_{0p}^2+w_{0x}^2)(y_{0p}^2+w_{0y}^2)} = \frac{\pi}{2w_{0x}^2 w_{0y}^2} \sum_{m=0}^{N} \sum_{n=0}^{N} a_{2m} a_{2n} H_{2m}\left(\frac{x_{0p}}{w_{0x}}\right) H_{2n}\left(\frac{y_{0p}}{w_{0y}}\right) \exp\left(-\frac{x_{0p}^2}{w_{0x}^2} - \frac{y_{0p}^2}{w_{0y}^2}\right), \quad (4.4)$$

Where the number of expansion is N, the weight coefficients are given as a_{2m} and a_{2n} 2mth order Hermite polynomial is given as $H_{2m}(.)$ and the 2nth order Hermite polynomial is given as $H_{2n}(.)$ [69]. Now, Eq. (4.1.2) can be rewritten as:

$$\mathrm{E}(x_{0s}, y_{0s}, 0) = \frac{\pi}{2w_{0x} w_{0y}} \sum_{m=0}^{N} \sum_{n=0}^{N} a_{2m} a_{2n} H_{2m}\left(\frac{x_{0s}}{w_{0x}}\right) H_{2n}\left(\frac{y_{0s}}{w_{0y}}\right) \exp\left(-\frac{x_{0s}^2}{w_{0x}^2} - \frac{y_{0s}^2}{w_{0y}^2}\right), \quad (4.5)$$

Where,

$$\frac{1}{w_j^2} = \frac{1}{w_0^2} + \frac{1}{2w_{0j}^2}, \quad (4.6)$$

and $j = x \text{ or } y$. The generalized Huygens-Fresnel diffraction integral is used to describe propagation of partially coherent Lorentz-Gauss beam through paraxial *ABCD* optical system:

$$\Gamma(\mathrm{x_a}, \mathrm{x_b}; \mathrm{y_a}, \mathrm{y_b}; \mathrm{z}) = -\frac{1}{\lambda B} \exp\left(\frac{ikD}{2B}\left[(x_b^2 + y_b^2) - (x_a^2 + y_a^2)\right]\right) \int_{-\infty}^{\infty}\int_{-\infty}^{\infty}\int_{-\infty}^{\infty}\int_{-\infty}^{\infty} \Gamma(x_{0a}, x_{0b}; y_{0a}, y_{0b}; z) \times \exp\left\{\frac{\mathrm{ik}}{2\mathrm{B}}\left[\begin{array}{c}\mathrm{A}\left(\mathrm{x_{0b}^2} + \mathrm{y_{0b}^2}\right) - \mathrm{A}(\mathrm{x_{0a}^2} + \mathrm{y_{0a}^2}) - 2(\mathrm{x_{0b}x_b} + \mathrm{y_{0b}y_b}) \\ +2(\mathrm{x_{0a}x_a} + \mathrm{y_{0a}y_a})\end{array}\right]\right\} \mathrm{d\,x_{0a} dx_{0b} dy_{0a} dy_{0b}}, \quad (4.7)$$

Wave number is given as $k = 2\pi/\lambda$, where λ is wavelength. It is considered that there is no endogenous aperture between source plane and output plane. Hence, *A*, *B*, *C* and *D* are real integers. Where, *A*, *B*, *C* and *D* are the matrix components of optical system between source plane and output plane.

The mathematical formulae stated as follows are used to calculate the mutual coherence function [70]:

$$\int_{-\infty}^{\infty} H_{2m'}(x)\exp[-(x-y)^2/v]\,dx = \sqrt{\pi/v}\,(1-v)^{m'} H_{2m'}[(1-v)^{-1/2}y], \tag{4.8}$$

$$H_{2m}(x) = \sum_{l=0}^{\infty} \frac{(-1)^l (2m)!}{l!(2m-2l)!}(2x)^{(2m-2l)}, \tag{4.9}$$

$$\int_{-\infty}^{\infty} x^{2n}\exp(-bx^2+2cx)dx = (2n)!\sqrt{\frac{\pi}{b}}\left(\frac{c}{b}\right)^{2n}\exp\left(\frac{c^2}{b}\right)\sum_{s=0}^{n}\frac{1}{s!(2n-2s)!}\left(\frac{b}{4c^2}\right)^{s}, \tag{4.10}$$

$\Gamma(x_a,x_b;y_a,y_b;z)$ (i.e. mutual coherence function) of partially coherent LGB in the output plane is,

$$\Gamma(x_a,x_b;y_a,y_b;z) = \Gamma(x_a,x_b,z)\,\Gamma(y_a,y_b,z)\,, \tag{4.11}$$

here $\Gamma(x_a,x_b,z)$ and $\Gamma(y_a,y_b,z)$ is defined as,

$$\Gamma(j_a,j_b,z) = \frac{\pi^2}{2}\sqrt{\frac{i}{\lambda B\alpha_{1j}\alpha_{2j}}}\exp\left(\frac{\beta_j^2}{\alpha_{2j}} - \frac{k^2 w_{0j}^2 j_2^2}{4\alpha_{1j}B^2} + \frac{ikD}{2B}(j_2^2 - j_1^2)\right)\sum_{m=0}^{N}\sum_{m'=0}^{N} a_{2m}a_{2m'}\left(1 - \frac{1}{\alpha_{1j}}\right)^{m'} \times \sum_{l_1=0}^{m}\frac{(-1)^{l_1}(2m)!}{l_1!(2m-2l_1)!}\sum_{l_2=0}^{m'}\frac{(-1)^{l_2}(2m')!}{l_2!(2m'-2l_2)!}\sum_{l_3=0}^{2m'-2l_2}\binom{2m'-2l_2}{l_3}2^{2(m+m')-2l_1-2l_2}\gamma_j^{l_3}\delta_j^{2m'-2l_2-l_3}$$

$$\times (2m+l_3-2l_1)!\left(\frac{\beta_j}{\alpha_{2j}}\right)^{2m+l_3-2l_1}\sum_{s=0}^{[m-l_1+l_3/2]}\frac{1}{s!(2m+l_3-2l_1-2s)!}\left(\frac{\alpha_{2j}}{4\beta_j^2}\right)^{s}, \tag{4.12}$$

Where $[m-l_1+l_3/2]$ will yield the greatest integer whose value is less than or equal to $(m-l_1+l_3/2)$, and

$$\alpha_{1j} = \left(\frac{1}{w_j^2} + \frac{1}{2\sigma_j^2} - \frac{ikA}{2B}\right)w_{0j}^2\,,\ \alpha_{2j} = \left(\frac{1}{w_j^2} + \frac{1}{2\sigma_j^2} + \frac{ikA}{2B}\right)w_{0j}^2 - \frac{w_{0j}^4}{4\alpha_{1j}\sigma_j^4}\,, \tag{4.13}$$

$$\beta_j = \frac{ikw_{0j}j_1}{2B} - \frac{ikw_{0j}^3 j_2}{2\alpha_{1j}B\sigma_j^2}\,,\ \gamma_j = \frac{w_{0j}^2}{2(\alpha_{1j}^2-\alpha_{1j})^{1/2}\sigma_j^2}\,,\ \delta_j = \frac{kw_{0j}j_2}{2iB(\alpha_{1j}^2-\alpha_{1j})^{1/2}}\,, \tag{4.14}$$

4.2.1 (a) Calculation for Spatial Degree of Coherence:

The spatial complex degree of coherence for incompletely coherent LGB is calculated on two reference points (x_a,y_a,z) and (x_b,y_b,z) and it is found out to be [64,33],

$$\mu(x_a,x_b;y_a,y_b;z) = \mu\,(x_a,x_b,z)\,\mu(y_a,y_b,z)\,, \tag{4.15}$$

where, $\mu\,(x_a,x_b,z)$ and $\mu(y_a,y_b,z)$ is given by,

$$\Gamma\,(j_a,j_b,z) = \frac{\Gamma(j_a,j_b,z)}{[\Gamma(j_a,j_a,z)\Gamma(j_b,j_b,z)]^{1/2}}\,, \tag{4.16}$$

The spatial complex degree of coherence is calculated by inserting Eq. (4.12) into Eq. (4.16).

4.2.1 (b) Calculation for Effective Beam Size:

The Effective beam size for partially coherent LGB in x and y directions of output plane is defined as [64]

$$W_{jz}=\sqrt{\frac{2\int_{-\infty}^{\infty}\int_{-\infty}^{\infty} j^2\Gamma(xa,xb:ya,yb;z)dxdy}{\int_{-\infty}^{\infty}\int_{-\infty}^{\infty}\Gamma(xa,xb:ya,yb;z)dxdy}}, \tag{4.17}$$

Inserting equation (4.12) into equation (4.17), we found out the expression of Effective beam size as;

$$W_{jz}=\sqrt{\frac{2\Omega_{1j}}{\Omega_{2j}}}\ , \tag{4.18}$$

With Ω_{1j} and Ω_{2j} given by,

$$\Omega_{1j}\ =$$

$$\sum_{m=0}^{N}\sum_{m'=0}^{N} a_{2m}a_{2m'}\left(1\ \ \frac{1}{\alpha_{1j}}\right)^{m'}\sum_{l_1=0}^{m}\frac{(-1)^{l_1}(2m)!}{l_1\,!(2m-2l_1)!}\sum_{l_2=0}^{m'}\frac{(-1)^{l_2}(2m')!}{l_2\,!(2m'-2l_2)!}\sum_{l_3=0}^{2m'-2l_2}\binom{2m'-2l_2}{l_3}\times$$

$$2^{2(m+m')-2l_1-2l_2}\gamma_j^{l_3}\xi_j^{2m'-2l_2-l_3}(2m+l_3-2l_1)!\sum_{s=0}^{[m-l_1+l_3/2]}\frac{1}{s!(2m+l_3-2l_1-2s)!4^s}\times$$

$$\alpha_{2j}^{2l_1+s-2m-l_3}\eta_j^{2m+l_3-2l_1-2s}\Gamma(\mathrm{m}+m'-l_1-l_2-s+1.5)\zeta_j^{l_1+l_2+s-m-m'-1.5}\ , \tag{4.19}$$

$$\Omega_{1j}\ =$$

$$\sum_{m=0}^{N}\sum_{m'=0}^{N} a_{2m}a_{2m'}\left(1\ \ \frac{1}{\alpha_{1j}}\right)^{m'}\sum_{l_1=0}^{m}\frac{(-1)^{l_1}(2m)!}{l_1\,!(2m-2l_1)!}\sum_{l_2=0}^{m'}\frac{(-1)^{l_2}(2m')!}{l_2\,!(2m'-2l_2)!}\sum_{l_3=0}^{2m'-2l_2}\binom{2m'-2l_2}{l_3}\times$$

$$2^{2(m+m')-2l_1-2l_2}\gamma_j^{l_3}\xi_j^{2m'-2l_2-l_3}(2m+l_3-2l_1)!\sum_{s=0}^{[m-l_1+l_3/2]}\frac{1}{s!(2m+l_3-2l_1-2s)!4^s}\times$$

$$\alpha_{2j}^{2l_1+s-2m-l_3}\eta_j^{2m+l_3-2l_1-2s}\Gamma(\mathrm{m}+m'-l_1-l_2-s+0.5)\zeta_j^{l_1+l_2+s-m-m'-0.5}\ , \tag{4.20}$$

Where, $\xi_j=\frac{kw_{0j}}{2iB(\alpha_{1j}^2-\alpha_{1j})^{1/2}}$, $\eta_j=\frac{ikw_{0j}}{2B}-\frac{ikw_{0j}{}^3}{4\alpha_{1j}B\sigma_j^2}$, $\zeta_j=\frac{k^2w_{0j}^2}{4\alpha_{1j}B^2}-\frac{\eta_j^2}{\alpha_{2j}}$, (4.21)

and $\Gamma(.)$ is a Gamma function.

4.2.2 Hermite-Gaussian Beams:

The propagation axis is assumed to be z-axis in Cartesian coordinate system. $\Gamma(x_{0a},x_{0b};y_{0a},y_{0b};0)$ is characterized as the function for mutual coherence of partially coherent HGB in the plane z=0 and is defined as,

$$\Gamma(x_{0a},x_{0b};y_{0a},y_{0b};0) = \mathrm{E}(x_{0a},y_{0a},0) \times \mathrm{E}(x_{0b},y_{0b},0) \times \mathrm{g}(x_{0a},x_{0b};y_{0a},y_{0b};0)\,, \tag{4.22}$$

Where $\mathrm{E}(x_{0a},y_{0a},0)$, $\mathrm{E}(x_{0b},y_{0b},0)$ and $\mathrm{g}(x_{0a},x_{0b};y_{0a},y_{0b};0)$ are given as,

$$\mathrm{E}(x_{0s},y_{0s},0) = \mathrm{H}_{2m}\left(\frac{\mathrm{x_{0s}}}{\mathrm{w_{0x}}}\right)\mathrm{H}_{2n}\left(\frac{\mathrm{y_{0s}}}{\mathrm{w_{0y}}}\right) \times \exp\left(-\frac{x_{0s}^2+y_{0s}^2}{w_0^2}\right), \tag{4.23}$$

Where

$$\frac{1}{\mathrm{w_j^2}} = \frac{1}{\mathrm{w_0^2}} + \frac{1}{2\mathrm{w_{0j}^2}}, \tag{4.24}$$

$$\mathrm{g}(x_{0a},x_{0b};y_{0a},y_{0b};0) = \exp\left[-\frac{(x_{0a}-x_{0b})^2}{2\sigma_x^2} - \frac{(y_{0a}-y_{0b})^2}{2\sigma_y^2}\right], \tag{4.25}$$

The mutual coherence function of partially coherent Hermite-Gaussian beam in the output plane is defined as

$$\Gamma(x_a,x_b;y_a,y_b;z) = \Gamma(x_a,x_b,z)\,\Gamma(y_a,y_b,z)\,, \tag{4.26}$$

Where, $\Gamma(x_a,x_b,z)$ and $\Gamma(y_a,y_b,z)$ is given as,

$$\Gamma(j_a,j_b,z) = \frac{2w_{0x}w_{0y}}{\pi} \times \frac{1}{\sum_{m=0}^{N}\sum_{n=0}^{N} a_{2m}a_{2n}} \frac{\pi^2}{2}\sqrt{\frac{i}{\lambda B\alpha_{1j}\alpha_{2j}}} \times$$

$$exp\left(\frac{\beta_j^2}{\alpha_{2j}} - \frac{k^2w_{0j}^2j_2^2}{4\alpha_{1j}B^2} + \frac{ikD}{2B}(j_2^2 - j_1^2)\right)\sum_{m=0}^{N}\sum_{m'=0}^{N} a_{2m}a_{2m'}\left(1-\frac{1}{\alpha_{1j}}\right)^{m'} \times$$

$$\sum_{l_1=0}^{m}\frac{(-1)^{l_1}(2m)!}{l_1!(2m-2l_1)!}\sum_{l_2=0}^{m'}\frac{(-1)^{l_2}(2m')!}{l_2!(2m'-2l_2)!}\sum_{l_3=0}^{2m'-2l_2}\binom{2m'-2l_2}{l_3}2^{2(m+m')-2l_1-2l_2}\gamma_j^{l_3}\delta_j^{2m'-2l_2-l_3} \times$$

$$(2m+l_3-2l_1)!\left(\frac{\beta_j}{\alpha_{2j}}\right)^{2m+l_3-2l_1}\sum_{s=0}^{\left[m-l_1+\frac{l_3}{2}\right]}\frac{1}{s!(2m+l_3-2l_1-2s)!}\left(\frac{\alpha_{2j}}{4\beta_j^2}\right)^s, \tag{4.27}$$

Where j = x or y, $[\mathrm{m}-\mathrm{l}_1+\mathrm{l}_3/2]$ yields the greatest integer which is less than or equal to $(\mathrm{m}-\mathrm{l}_1+\mathrm{l}_3/2)$, and

$$\alpha_{1j}=\left(\frac{1}{\mathrm{w_j^2}}+\frac{1}{2\sigma_j^2}-\frac{\mathrm{ikA}}{2\mathrm{B}}\right)\mathrm{w_{0j}^2},\alpha_{2j}=\left(\frac{1}{\mathrm{w_j^2}}+\frac{1}{2\sigma_j^2}+\frac{\mathrm{ikA}}{2\mathrm{B}}\right)\mathrm{w_{0j}^2}-\frac{\mathrm{w_{0j}^4}}{4\alpha_{1j}\sigma_j^4}, \tag{4.28}$$

$$\beta_j=\frac{\mathrm{ikw_{0j}j_1}}{2\mathrm{B}}-\frac{\mathrm{ikw_{0j}^3j_2}}{2\alpha_{1j}\mathrm{B}\sigma_j^2},\gamma_j = \frac{\mathrm{w_{0j}^2}}{2(\alpha_{1j}^2-\alpha_{1j})^{1/2}\sigma_j^2},\ \delta_j = \frac{\mathrm{kw_{0j}j_2}}{2\mathrm{iB}(\alpha_{1j}^2-\alpha_{1j})^{1/2}}, \tag{4.29}$$

4.2.2 (a) Calculation for Spatial Degree of Coherence:

The spatial complex degree of coherence for partially coherent HGB is calculated at two reference points (x_a,y_a,z) and (x_b,y_b,z) and it is found out to be [64,33],

$$\mu(x_a,x_b;y_a,y_b;z) = \mu\,(x_a,x_b,z)\,\mu(y_a,y_b,z)\,, \tag{4.30}$$

where, $\mu\ (x_a, x_b, z)$ and $\mu(y_a, y_b, z)$ is given by,

$$\Gamma\ (j_a, j_b, z) = \frac{\Gamma(j_a, j_b, z)}{[\Gamma(j_a, j_a, z)\Gamma(j_b, j_b, z)]^{1/2}}\ , \tag{4.31}$$

The spatial complex degree of coherence is calculated by inserting Eq. (4.27) into Eq. (4.31).

4.2.2 (b) Calculation for Effective Beam Size:

Effective beam size for partially coherent HGB in x and y directions of output plane is defined as [64]

$$W_{jz} = \sqrt{\frac{2\int_{-\infty}^{\infty}\int_{-\infty}^{\infty} j^2\Gamma(xa,xb:ya,yb;z)dxdy}{\int_{-\infty}^{\infty}\int_{-\infty}^{\infty}\Gamma(xa,xb:ya,yb;z)dxdy}}, \tag{4.32}$$

Inserting equation (4.27) into equation (4.32), we found out the expression of Effective beam size as;

$$W_{jz} = \sqrt{\frac{€_1}{€_2}}\ , \tag{4.33}$$

Where

$$€_1 = \frac{k^2}{4\pi^2 z^2} w_0^2 \sqrt{\frac{\pi}{e_1}} \left(1 - \frac{1}{e_1}\right)^{m/2} \sum_{j_1=0}^{\left[\frac{m}{2}\right]} \frac{(-1)^{j_1} m!}{j_1!(m-2j_1)!} \sum_{l_1=0}^{\left[\frac{m}{2}\right]} \frac{(-1)^{l_1} m!}{l_1!(m-2l_1)!} \sum_{t_1=0}^{m-2l_1} \binom{m-2l_1}{t_1} \times$$

$$(2)^{2m-2j_1-2l_1} (g_1)^{t_1} (m + t_1 - 2j_1)! \sqrt{\frac{\pi}{e_2}} \sum_{q_1=0}^{\left[\frac{m+t_1-2j_1}{2}\right]} \frac{1}{q_1!(m+t_1-2j_1-2q_1)!} \left(\frac{1}{e_2}\right)^{m+t_1-2j_1} \times$$

$$\left(\frac{e_2}{4}\right)^{q_1} (f_2)^{m+t_1-2j_1-2q_1} (-h_2)^{m-t_1-2l_1} \times \frac{\Gamma\left(\frac{2m-2l_1-2j_1-2q_1+3}{2}\right)}{\sqrt{\left(\frac{k^2 w_0^2}{4e_1 z^2} - \frac{f_2^2}{e_2}\right)^{2m-2l_1-2j_1-2q_1+3}}}\ , \tag{4.34}$$

$$€_2 = \frac{k^2}{4\pi^2 z^2} w_0^2 \sqrt{\frac{\pi}{e_1}} \left(1 - \frac{1}{e_1}\right)^{m/2} \sum_{j_1=0}^{\left[\frac{m}{2}\right]} \frac{(-1)^{j_1} m!}{j_1!(m-2j_1)!} \sum_{l_1=0}^{\left[\frac{m}{2}\right]} \frac{(-1)^{l_1} m!}{l_1!(m-2l_1)!} \sum_{t_1=0}^{m-2l_1} \binom{m-2l_1}{t_1} \times$$

$$(2)^{2m-2j_1-2l_1} (g_1)^{t_1} (m + t_1 - 2j_1)! \sqrt{\frac{\pi}{e_2}} \sum_{q_1=0}^{\left[\frac{m+t_1-2j_1}{2}\right]} \frac{1}{q_1!(m+t_1-2j_1-2q_1)!} \left(\frac{1}{e_2}\right)^{m+t_1-2j_1} \times$$

$$\left(\frac{e_2}{4}\right)^{q_1} (f_2)^{m+t_1-2j_1-2q_1} (-h_2)^{m-t_1-2l_1} \times \frac{\Gamma\left(\frac{2m-2l_1-2j_1-2q_1+1}{2}\right)}{\sqrt{\left(\frac{k^2 w_0^2}{4e_1 z^2} - \frac{f_2^2}{e_2}\right)^{2m-2l_1-2j_1-2q_1+1}}}\ , \tag{4.35}$$

Where, $f_2 = \frac{ikw_0}{2B} - \frac{w_0^3 ik}{4Be_1\sigma_j^2}$, $h_2 = \frac{ikw_0}{2B}\left(\frac{1}{e_1^2 - e_1}\right)^{1/2}$, $e_1 = 1 - \frac{ikw_0^2}{2B} + \frac{w_0^2}{2\sigma_j^2}$,

$$e_2 = 1 + \frac{ikw_0^2}{2B} + \frac{w_0^2}{2\sigma_j^2} - \frac{w_0^4}{4e_1\sigma_j^4}, \tag{4.36}$$

4.4 Numerical Problem

The partially coherent LGB is converted as converging beam by placing a thin lens whose focal length is f in front of single mode diode laser. Here, x and y directions are seperable therefore, only x-direction is considered in calculations given below. The case of free space propagation is considered in this work. The matrix components of the arrangement are taken as follows:

$$\begin{bmatrix} A & B \\ C & D \end{bmatrix} = \begin{bmatrix} 1 & 2f \\ 0 & 1 \end{bmatrix}$$

The parameters used are chosen as follow:

$\lambda = 0.8$ μm, (operating wavelength)

f = 1m, (focal length)

$x_a = 0.1$ mm, $x_b = 0.4$ mm (point of calculation)

When w_{0x} is variable, $w_0 = 2$ mm, (waist width of Gaussian part of both the beams)

When w_0 is variable, $w_{0x} = 2$ mm, (parameter associated with beam width of Lorentz and Hermite part corresponding to the beam in x-direction)

4.4.1 Lorentz-Gauss Beams:

4.4.1 (a) Spatial Complex Degree of Coherence

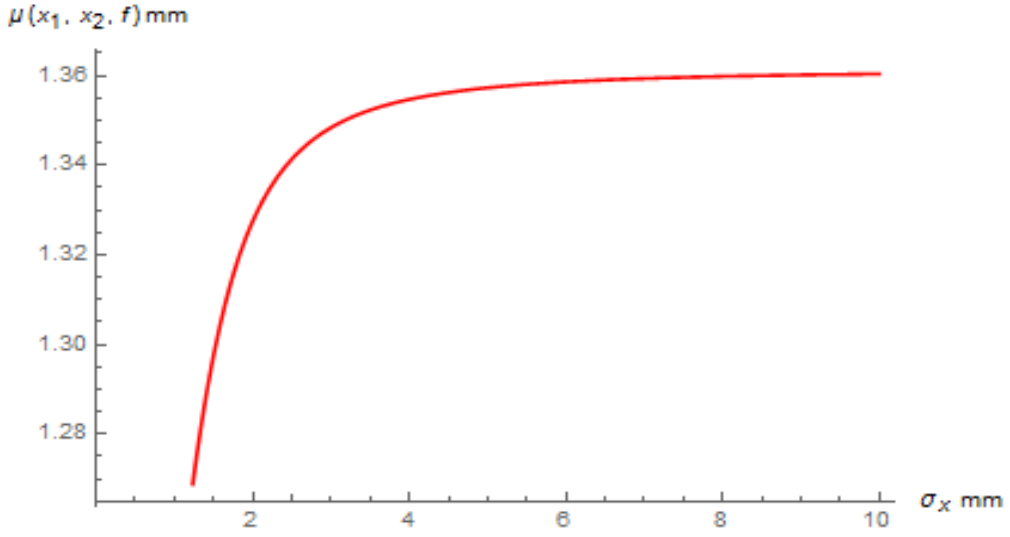

Figure 4.1 Spatial complex degree of coherence versus coherence length of partially coherent LGB in focal plane in x direction for $w_{0x} = 1$ mm.

Figure 4.1 shows that the Spatial complex degree of coherence has minimum value greater than 1 for w_{0x} = 1 mm but the maximum value is not much larger so the deviation shown by Spatial complex degree of coherence for coherence length ranging from 0.2 mm to 10 mm is very small.

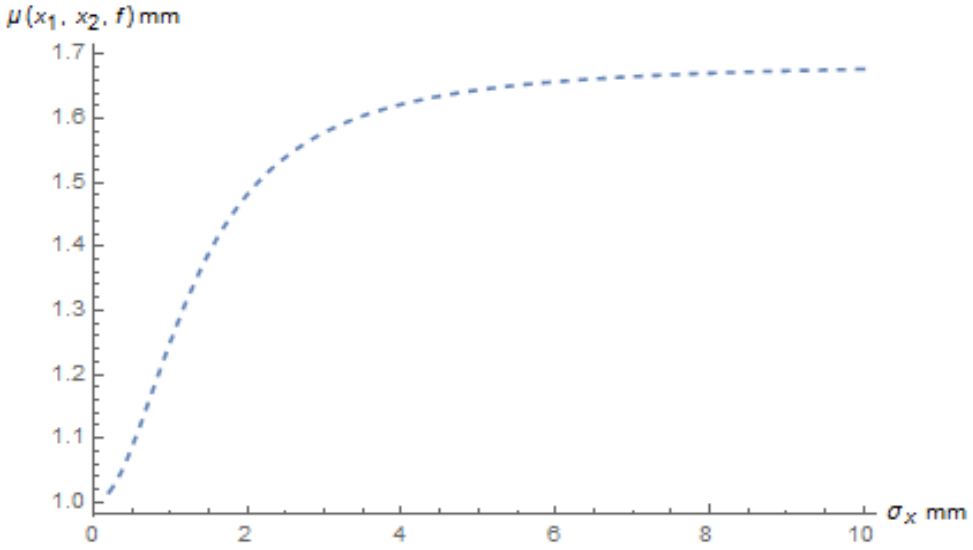

Figure 4.2 Spatial complex degree of coherence versus coherence length of partially coherent LGB in focal plane in x direction for w_{0x} = 2 mm.

Figure 4.2 shows that the Spatial complex degree of coherence has minimum value equal to 1 for w_{0x} = 2 mm but the deviation shown by Spatial complex degree of coherence from minimum to maximum value is larger than that for w_{0x} = 1 mm.

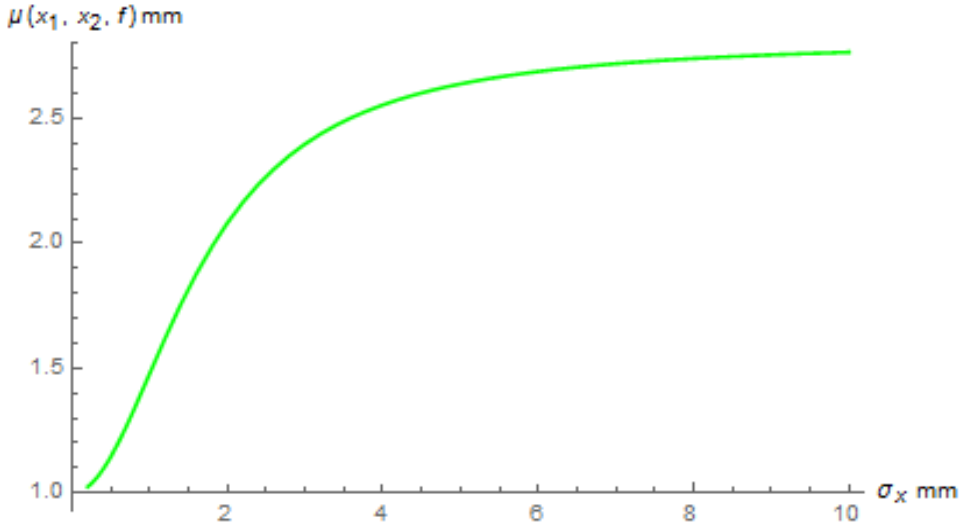

Figure 4.3 Spatial complex degree of coherence versus coherence length of partially coherent LGB in focal plane in x direction for w_{0x} = 3 mm.

Figure 4.3 shows that the Spatial complex degree of coherence has minimum value equal to 1 for w_{0x} = 3 mm but the deviation shown by Spatial complex degree of coherence from minimum to maximum value is larger than that for w_{0x} = 1 mm and w_{0x} = 2 mm.

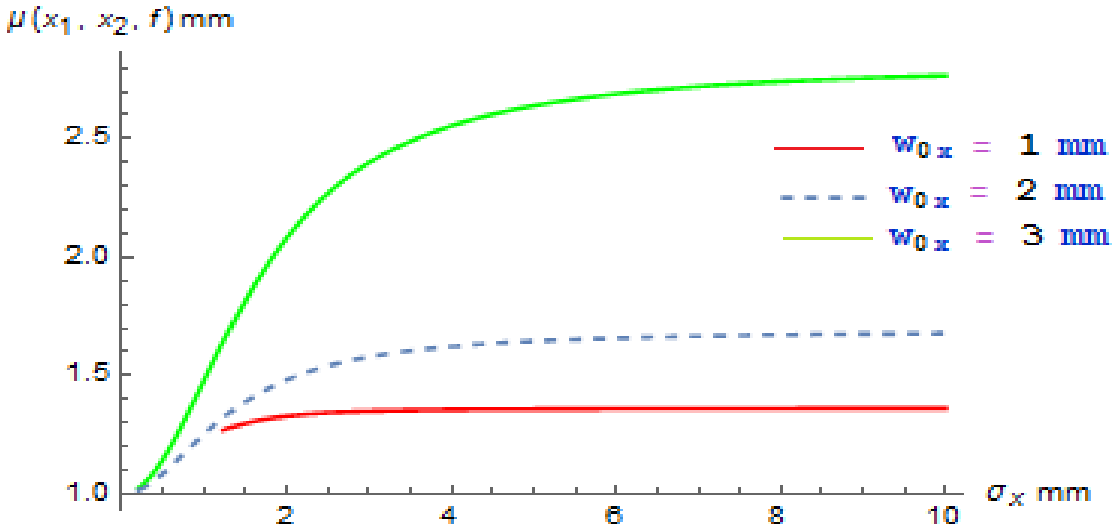

Figure 4.4 Spatial complex degree of coherence versus coherence length of partially coherent LGB in focal plane in x direction for w_0 = 2 mm.

From Figure 4.4 it is clearly evident that larger value of w_{0x} has larger Spatial complex degree of coherence and Spatial complex degree of coherence does not saturate for the maximum value 1 for unstable resonator.

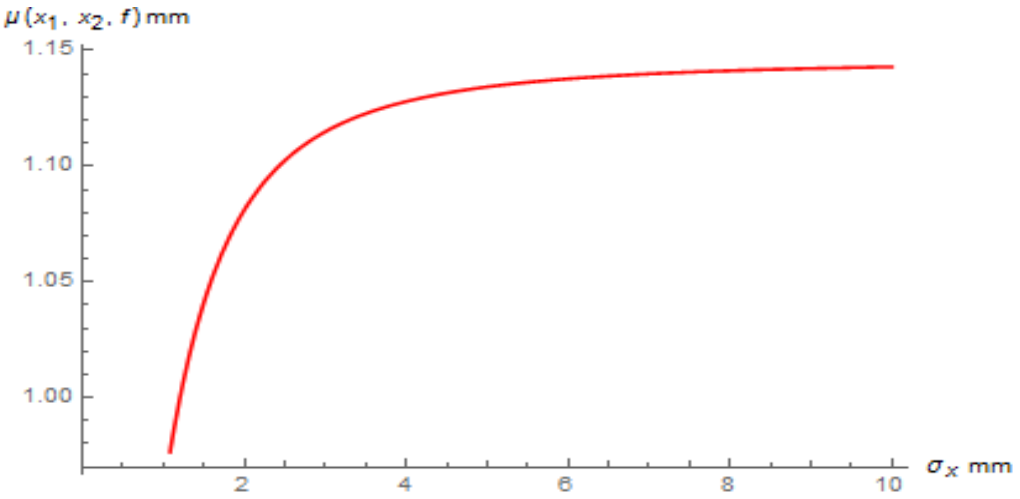

Figure 4.5 Spatial complex degree of coherence versus coherence length of partially coherent LGB in focal plane in x direction for w_0 = 1 mm.

.

From Figure 4.5 it is clear that when w_0 = 1 mm the minimum value of spatial complex degree of coherence is less than 1 and maximum value is also less than the value which is achieved when w_{0x} = 1 mm.

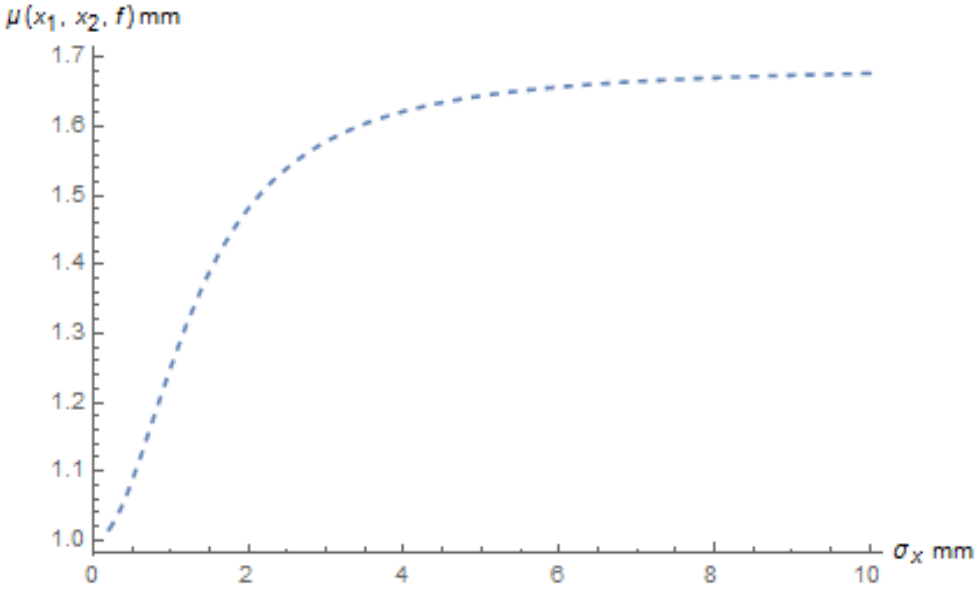

Figure 4.6 Spatial complex degree of coherence versus coherence length of partially coherent LGB in focal plane in x direction for w_0 = 2 mm.

As is evident from Figure 4.6, when w_0 = 2 mm the characteristics of spatial complex degree of coherence are same as that for w_{0x} = 2 mm.

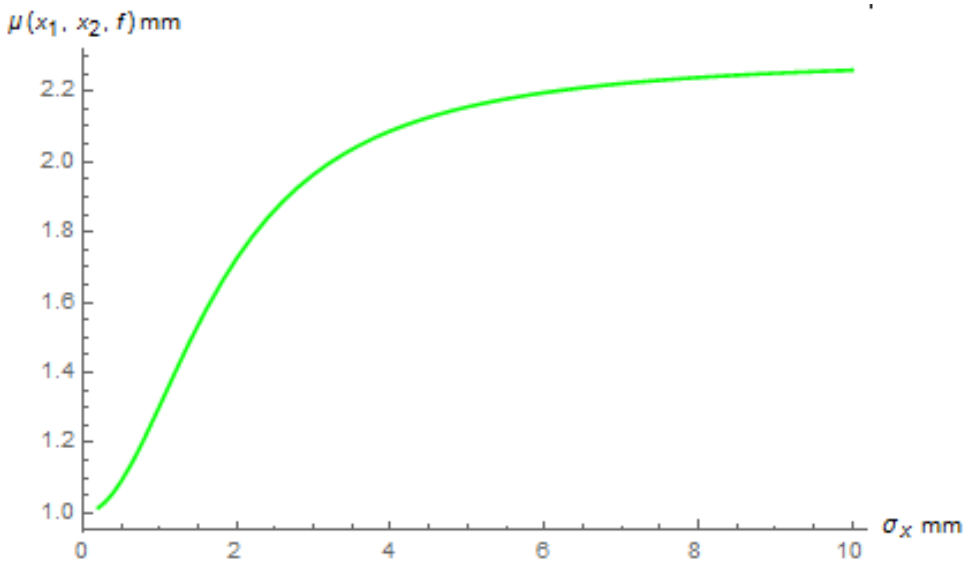

Figure 4.7 Spatial complex degree of coherence versus coherence length of partially coherent LGB in focal plane in x direction for w_0 = 3 mm.

The result in Figure 4.7 shows that as value of w_0 increases the maximum value of the curve of spatial complex degree of coherence increases but it remains less than the corresponding value of w_{0x}.

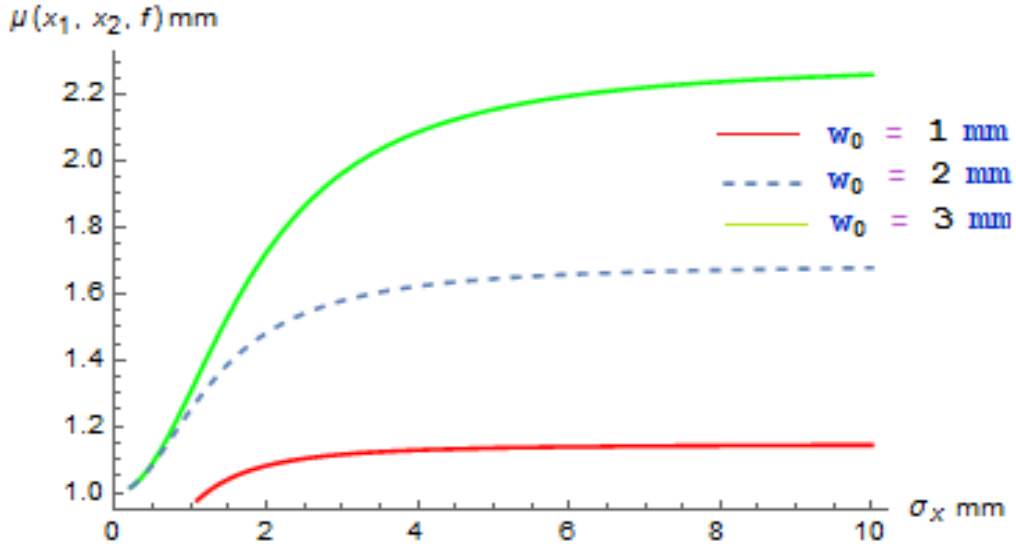

Figure 4.8 Spatial complex degree of coherence versus coherence length of partially coherent LGB in focal plane in x direction for $w_{0x} = 2$ mm.

.

From both the cases we found out that Spatial complex degree of coherence does not saturates for value 1 for unstable resonator as was the case for stable resonator. It implies that focal length plays very significant role in the propagation of optical beams. Its value is 1 for Gaussian beam so it should be as near to 1 as possible for other beams too.

The value of Spatial complex degree of coherence for Gaussian beam is 1 for the case of stable and unstable resonator. Whereas in case of Lorentz-Gauss beam for stable resonator the value of Spatial complex degree of coherence tends to saturate for value 1 as w_0 and w_{0x} increases but for unstable resonator its minimum value is greater than 1.

Therefore we can conclude that if the ratio of beam parameters to the wavelength is not significant than we should apply optical beams for smaller values of w_0 and w_{0x} for the case of unstable resonator because for smaller values of w_0 and w_{0x} the value of Spatial complex degree of coherence is nearer to 1.

4.4.1 (b) Effective Beam Size

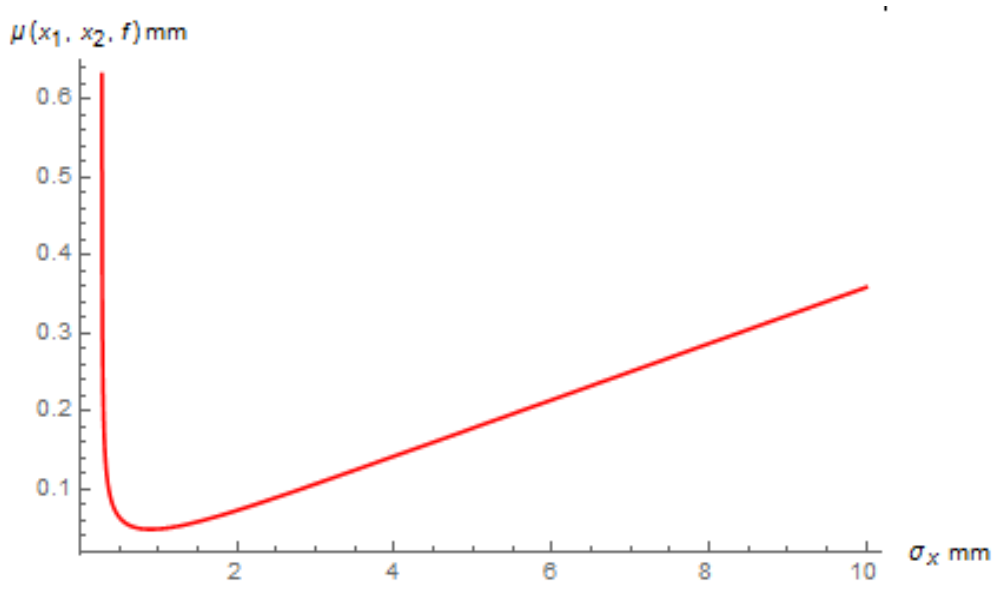

Figure 4.9 Effective Beam Size versus coherence length for partially coherent LGB in focal plane in x direction for w_{0x} = 1 mm.

It is apparent from the figure 4.9 that Effective beam size possesses maximum value for very small coherence length and then it is decreasing. There is a valley condition between coherence length value 0.1 to 2 mm after which the graph is increasing asymptotically.

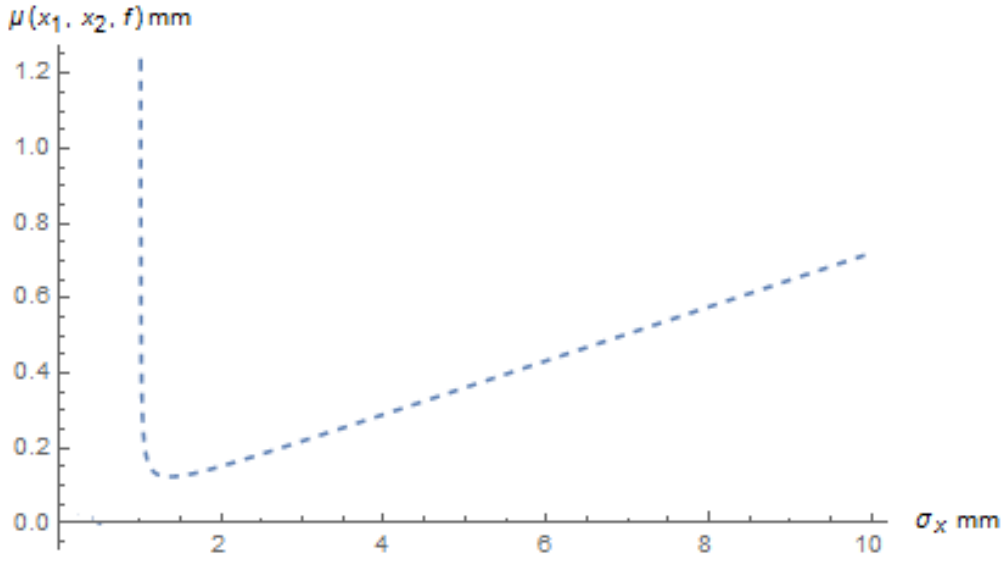

Figure 4.10 Effective Beam Size versus coherence length for partially coherent LGB in focal plane in x direction for w_{0x} = 2 mm.

Figure 4.10 shows the simliar characteristics as shown by Lorentz-Gauss beam for value of w_{0x} = 1 mm but the difference is in the magnitude of the maximum value of Effective beam size and the duration of threshold length. The threshold duration of coherence length is smaller for w_{0x} = 2 mm.

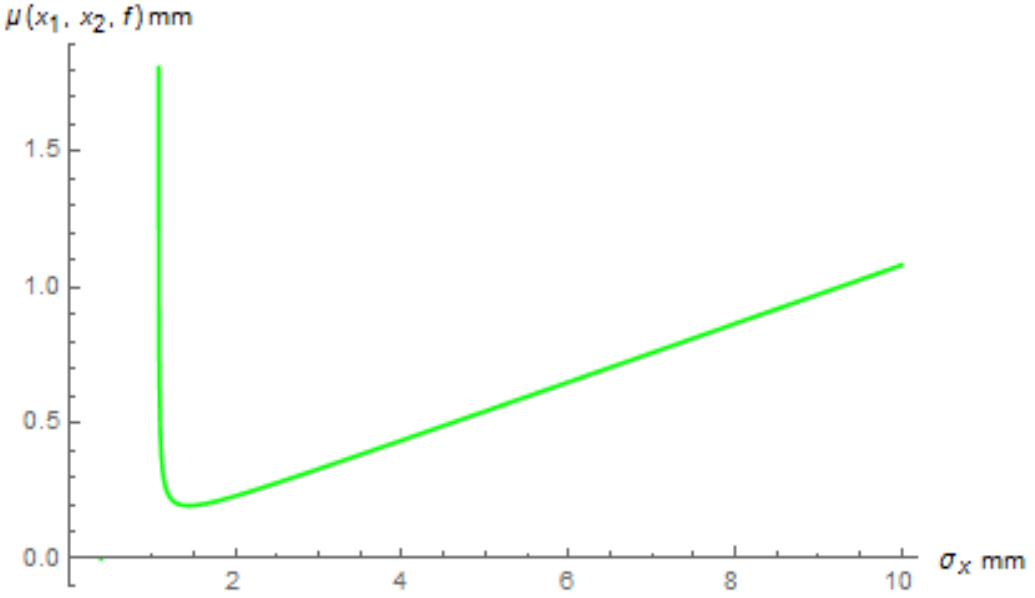

Figure 4. Effective Beam Size versus coherence length for partially coherent LGB in focal plane in x direction for w_{0x} = 3 mm.

Similarly when w_{0x} = 3 mm the maximum value attained by Effective beam size is highest. The threshold duration is smallest for this result.

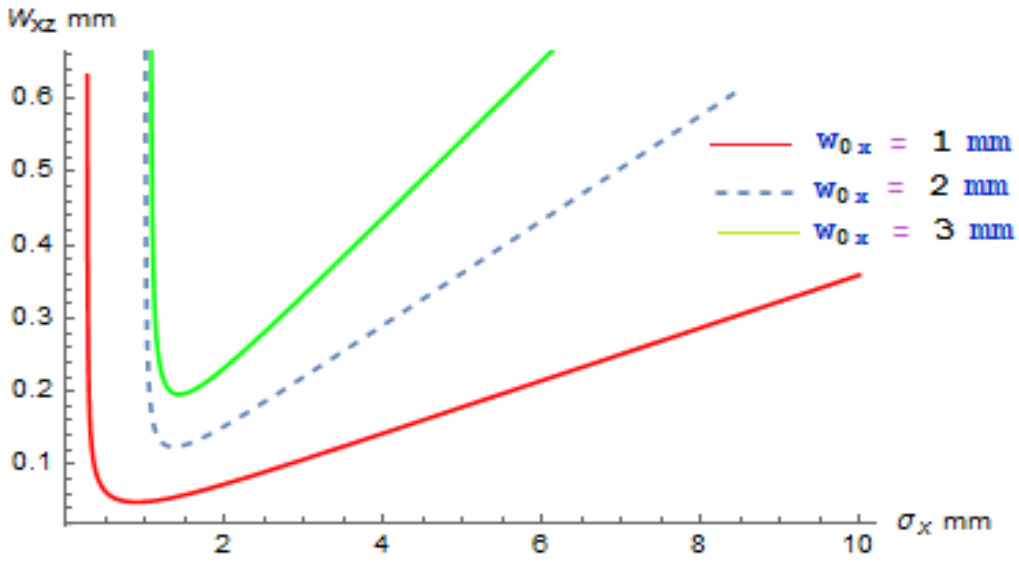

Figure 4.12 Effective Beam Size versus coherence length for partially coherent LGB in focal plane in x direction for w_0 = 2 mm.

Figure 4.12 clearly shows that as the value of w_{0x} increases the maximum value of Effective beam size increases and the duration of threshold length decreases or in other words the valley area decreases.

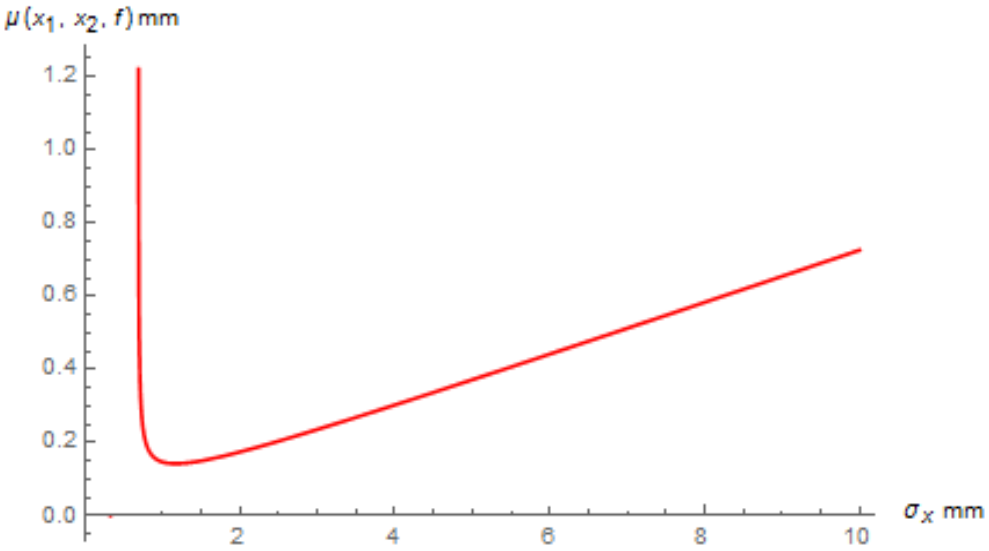

Figure 4.13 Effective Beam Size versus coherence length for partially coherent LGB in focal plane in x direction for $w_0 = 1$ mm.

Figure 4.13 shows that if compared with result obtained for $w_{0x} = 1$ mm the maximum value of Effective beam size is higher for the case of $w_0 = 1$ mm. Here, the valley condition is arising from 0.8 to 2 mm nearly whereas in case of $w_{0x} = 1$ mm it was from 0.1 mm to 2 mm.

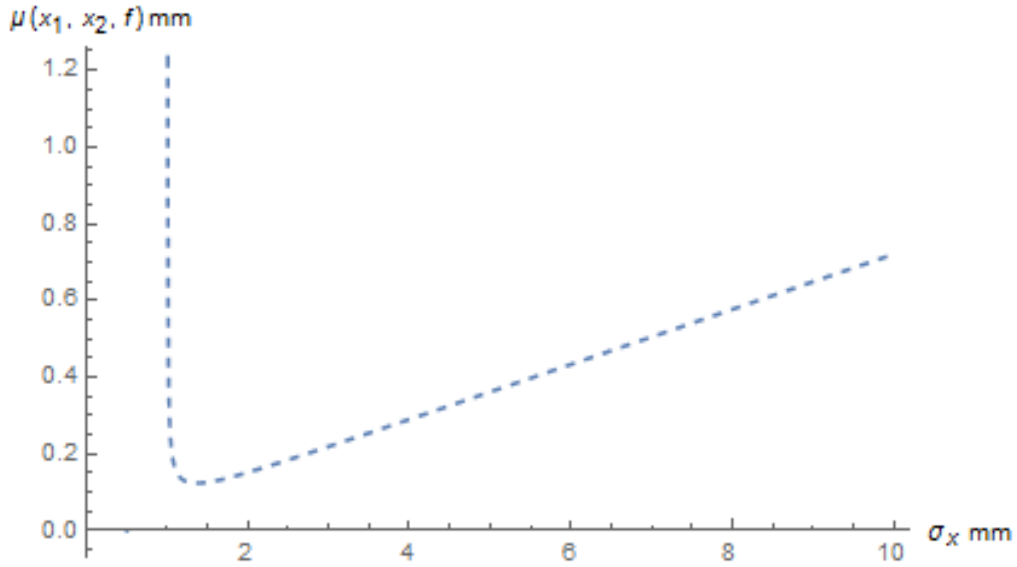

Figure 4.14 Effective Beam Size versus coherence length for partially coherent LGB in focal plane in x direction for $w_0 = 2$ mm.

The results obtained for the case of w_0 = 2 mm is similar to that of w_{0x} = 2 mm. The threshold point is greater than 0.8 mm for this case hence the valley condition is delayed as value of w_0 is increasing.

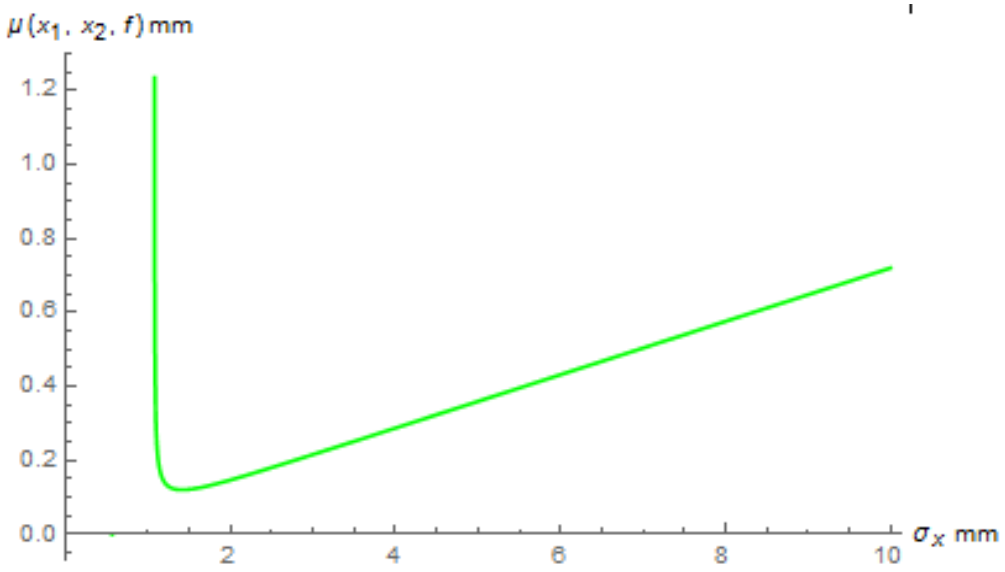

Figure 4.15 Effective Beam Size versus coherence length for partially coherent LGB in focal plane in x direction for w_0 = 3 mm.

The Effective beam size is not showing much difference when value of w_0 is further increased. In the case of varying w_{0x} the change in characteristics of Effective beam size is evident with increased value of w_{0x}, whereas it is not the case for variable w_0.

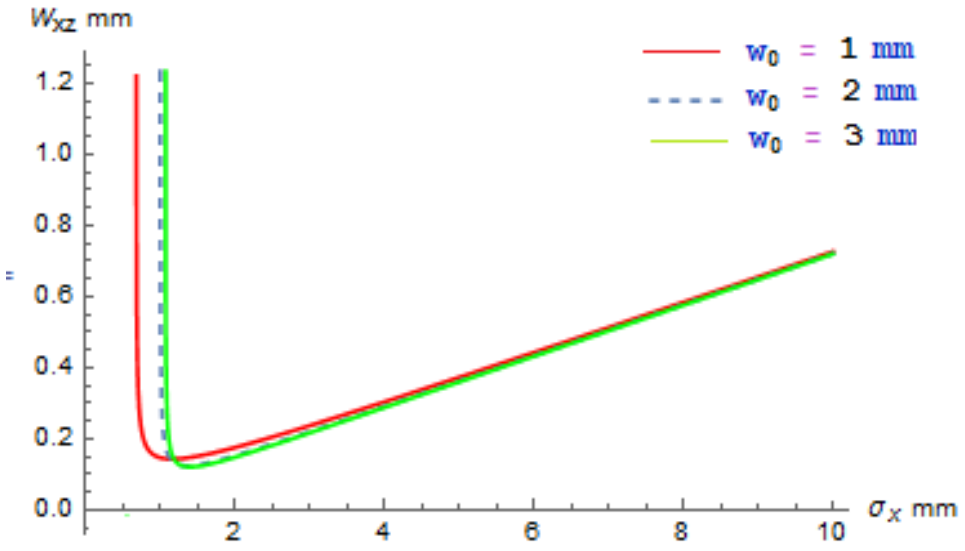

Figure 4.16 Effective Beam Size versus coherence length for partially coherent LGB in focal plane in x direction for w_{0x} = 2 mm.

We have found out through these results that for effective beam size of Lorentz-Gauss beams there exists a threshold point between coherence length values of 0.1 mm to 2 mm. The graphs between Effective Beam Size W_{xz} and Coherence Length σ_x reveal that the asymptotic behaviour with respect to effective beam size and exponence of convergence with respect to coherence length are proportional. For beam spot size w_{0x} = 1mm the asymptotic behaviour of effective beam size as well as exponence of convergence of Coherence length are minimum while these are maximum for w_{0x} = 3mm in our study.

The behaviour of Lorentz-Gauss beam is such that the maximum value of effective beam size attained by the beam for three different values of w_0 is same but for smaller values of w_0 it is attaining maximum value for smaller coherence length as compared to the larger values of w_0. As the value of w_0 increases the coherence length used to attain the maximum value of effective beam size is almost equal and the behaviour after threshold is asymptotic. Hence we can conclude that for larger values of w_0 there is no significant difference in behaviour of effective beam size of Lorentz-Gauss beams.

4.4.2 Hermite-Gaussian Beams:

4.4.2 (a) Spatial Complex Degree of Coherence

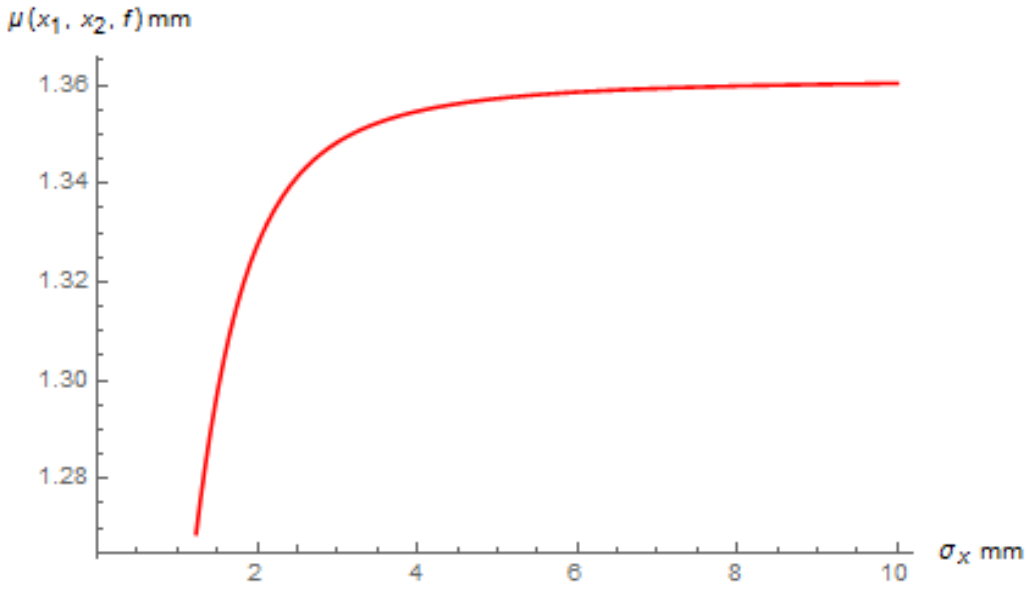

Figure 4.17 Spatial complex degree of coherence versus coherence length of partially coherent HGB in focal plane in x direction for w_{0x} = 1 mm.

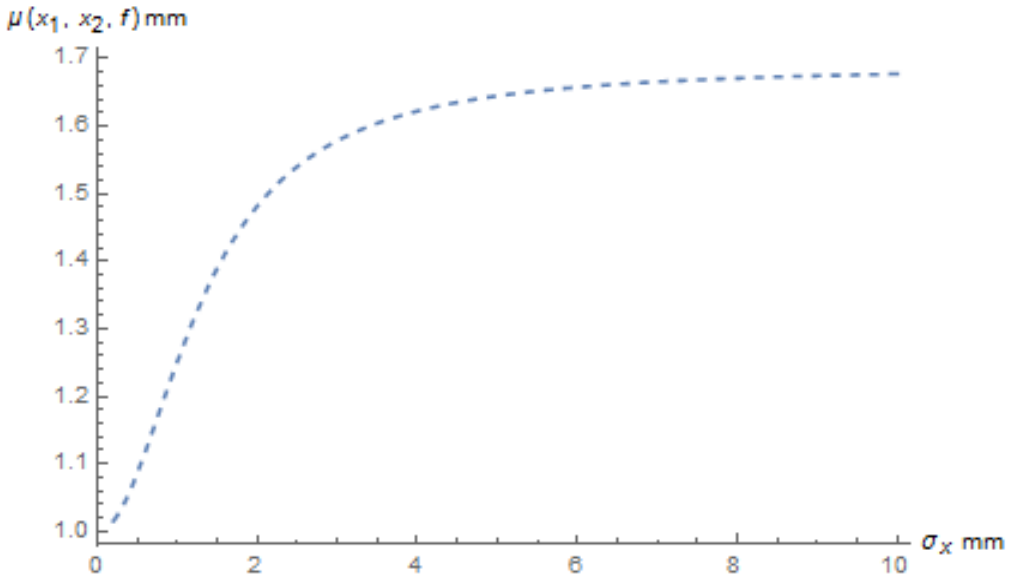

Figure 4.18 Spatial complex degree of coherence versus coherence length of partially coherent HGB in focal plane in x direction for w_{0x} = 2 mm.

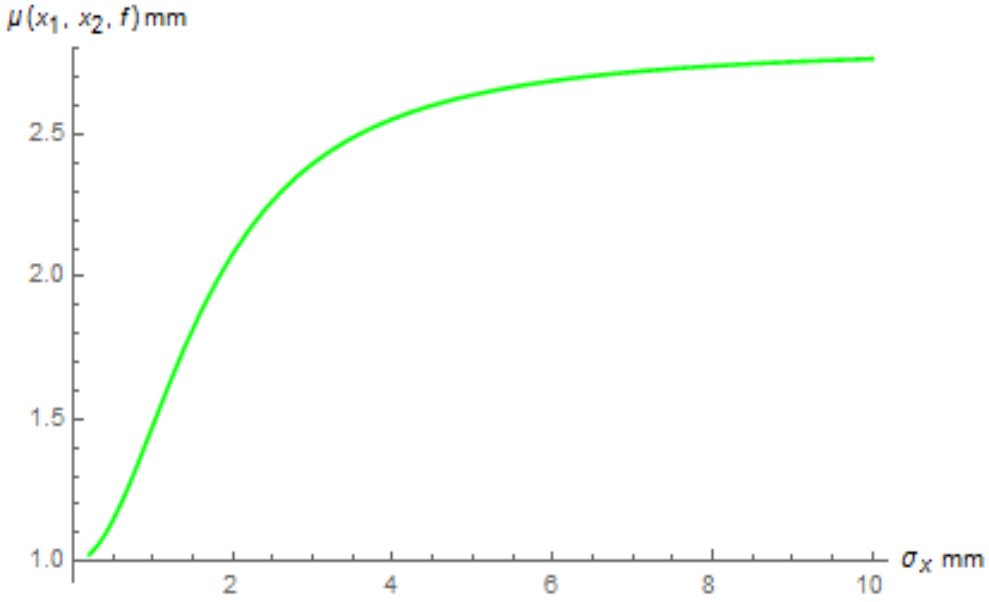

Figure 4.19 Spatial complex degree of coherence versus coherence length of partially coherent HGB in focal plane in x direction for w_{0x} = 3 mm.

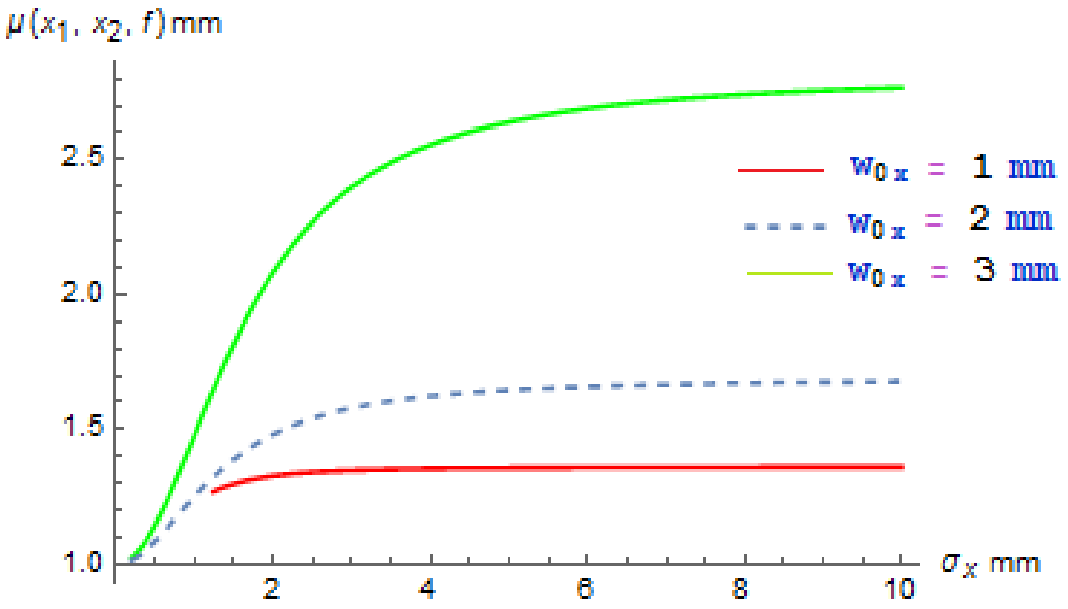

Figure 4.20 Spatial complex degree of coherence versus coherence length of partially coherent HGB in focal plane in x direction for $w_0 = 2$ mm.

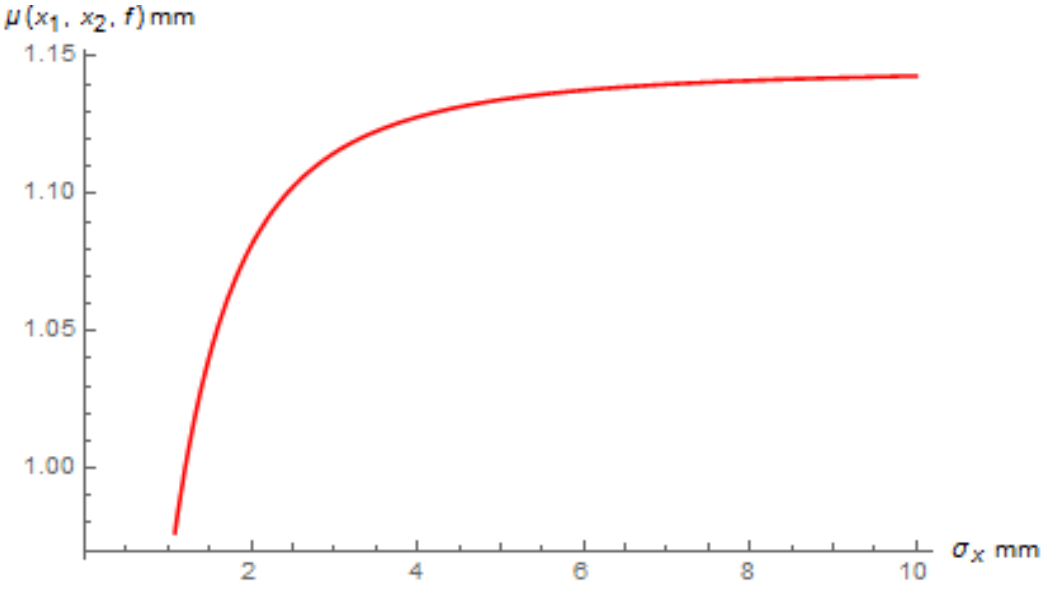

Figure 4.21 Spatial complex degree of coherence versus coherence length of partially coherent HGB in focal plane in x direction for $w_0 = 1$mm.

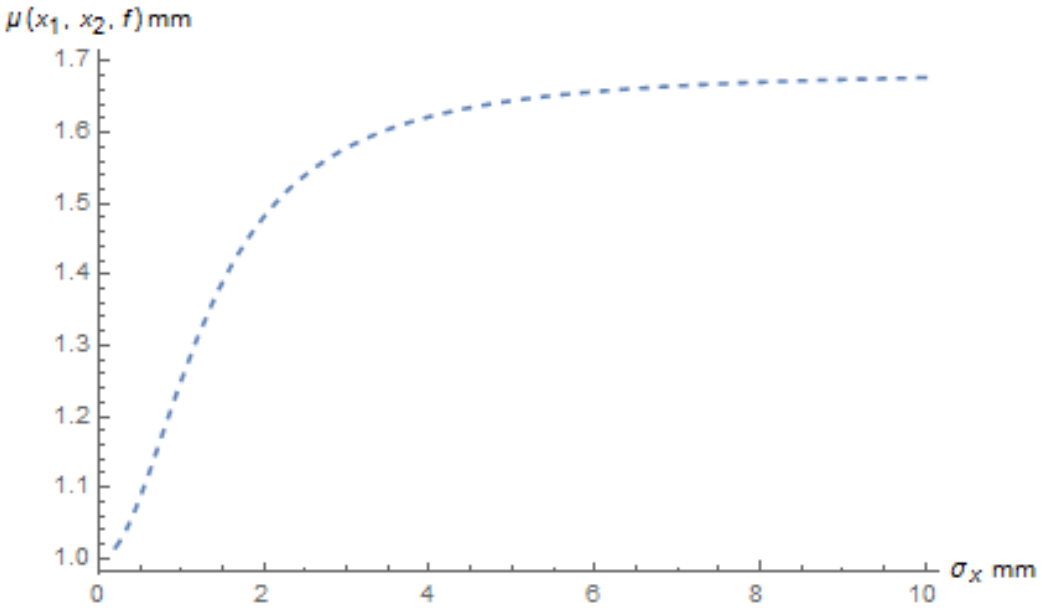

Figure 4.22 Spatial complex degree of coherence versus coherence length of partially coherent HGB in focal plane in x direction for $w_0 = 2$ mm.

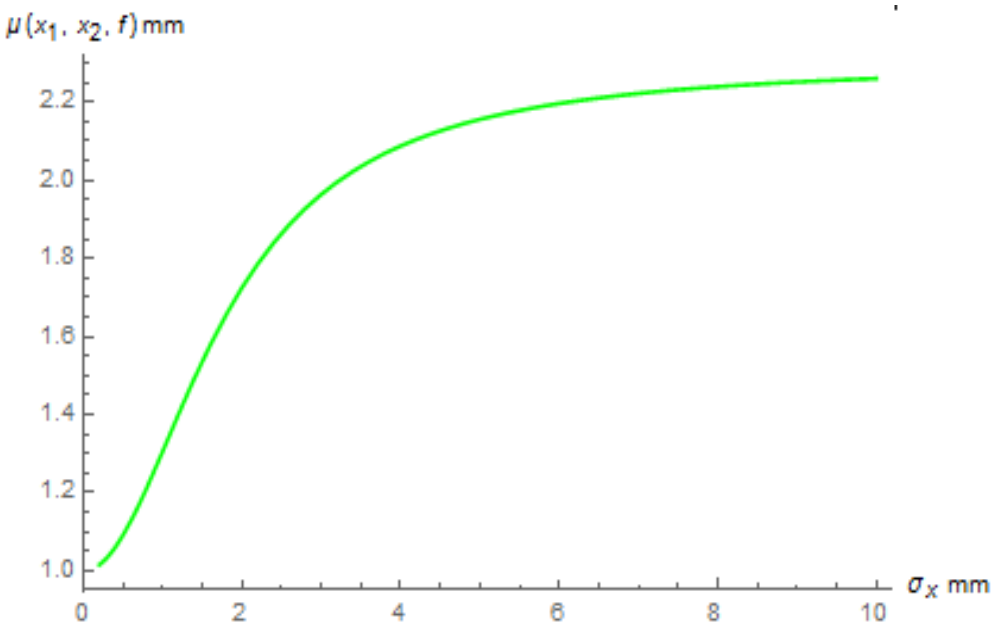

Figure 4.23 Spatial complex degree of coherence versus coherence length of partially coherent HGB in focal plane in x direction for $w_0 = 3$ mm.

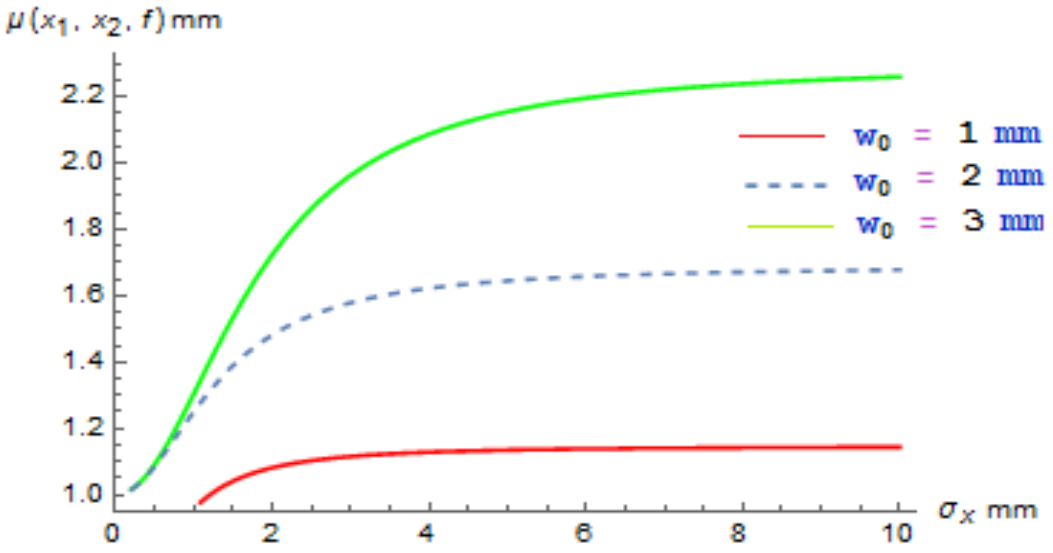

Figure 4.24 Spatial complex degree of coherence versus coherence length of partially coherent HGB in focal plane in x direction for w_{0x} = 2 mm.

As is evident from equations (5) and (21) electric fields of Lorentz-Gauss beam and Hermite-Gaussian beams differ by the value $\frac{\pi}{2w_{0x}^2 w_{0y}^2}\sum_{m=0}^{N}\sum_{n=0}^{N} a_{2m}a_{2n}$ which eventually does not affect the calculation for complex spatial degree of coherence therefore it comes out to be equal for the two beams. The results obtained satisfy the theory and are same for both the beams.

4.4.2 (b) Effective Beam Size

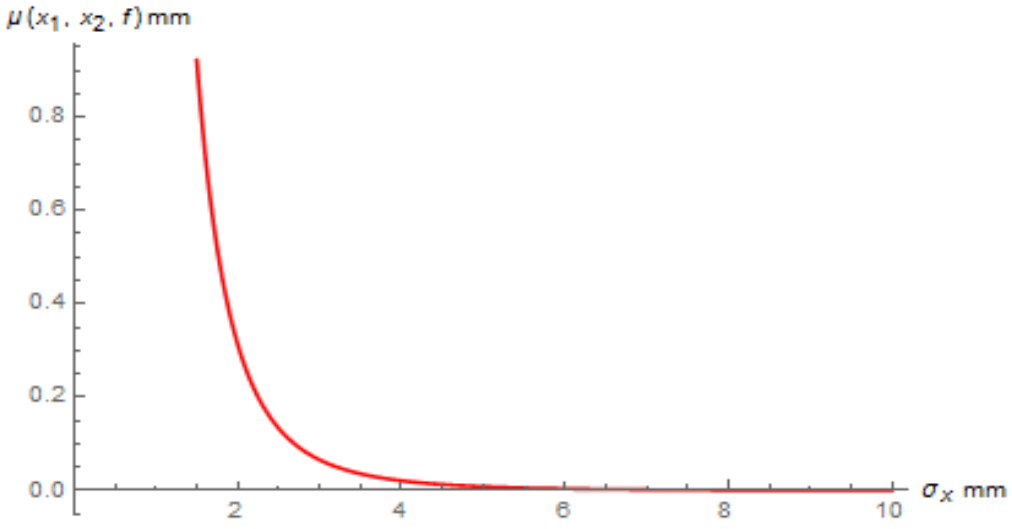

Figure 4.25 Effective Beam Size versus coherence length for partially coherent HGB in focal plane in x direction for w_{0x} = 1 mm.

It is shown in figure 4.25 that the Effective beam size is decreasing with increase in coherence length and after threshold point of nearly 6 mm it is diminishing to zero. This is in contrast to Lorentz-Gauss beam where a valley point is present after which Effective beam size increases.

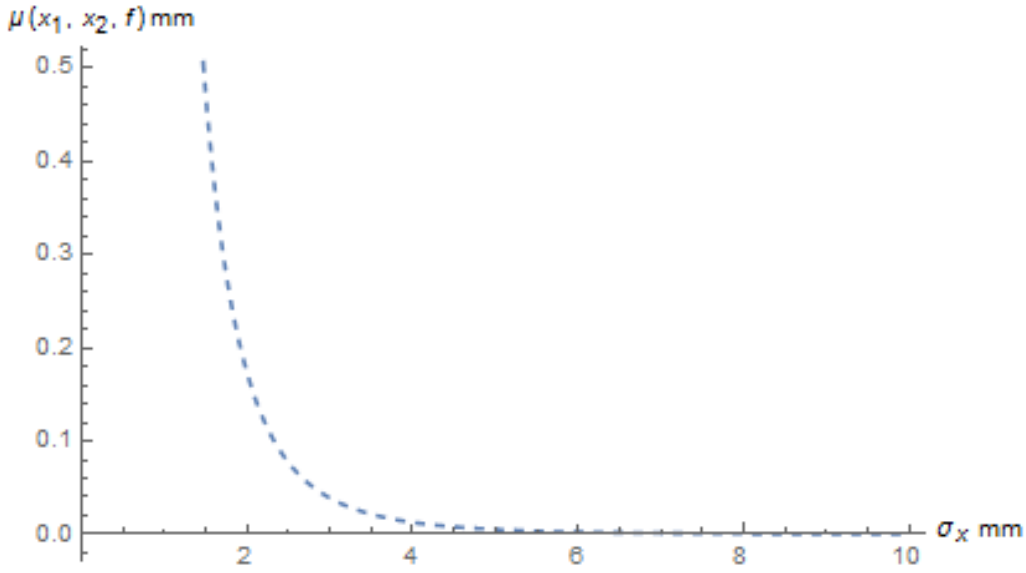

Figure 4.26 Effective Beam Size versus coherence length for partially coherent HGB in focal plane in x direction for w_{0x} = 2 mm.

It is clear from figure 4.26 that the maximum value attained by Effective beam size is less for w_{0x} = 2 mm as compared to that for w_{0x} = 1 mm and it is diminishing faster than the previous case.

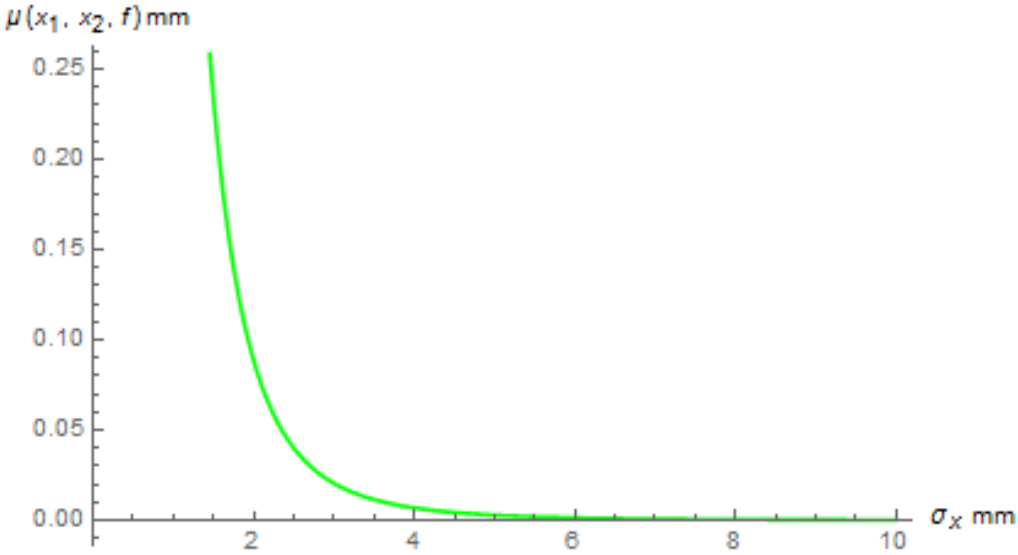

Figure 4.27 Effective Beam Size versus coherence length for partially coherent HGB in focal plane in x direction for w_{0x} = 3 mm.

It is evident from figure 4.27 that the maximum value of Effective beam size is decreasing with increasing value of w_{0x} and its rate of decrease is also increasing.

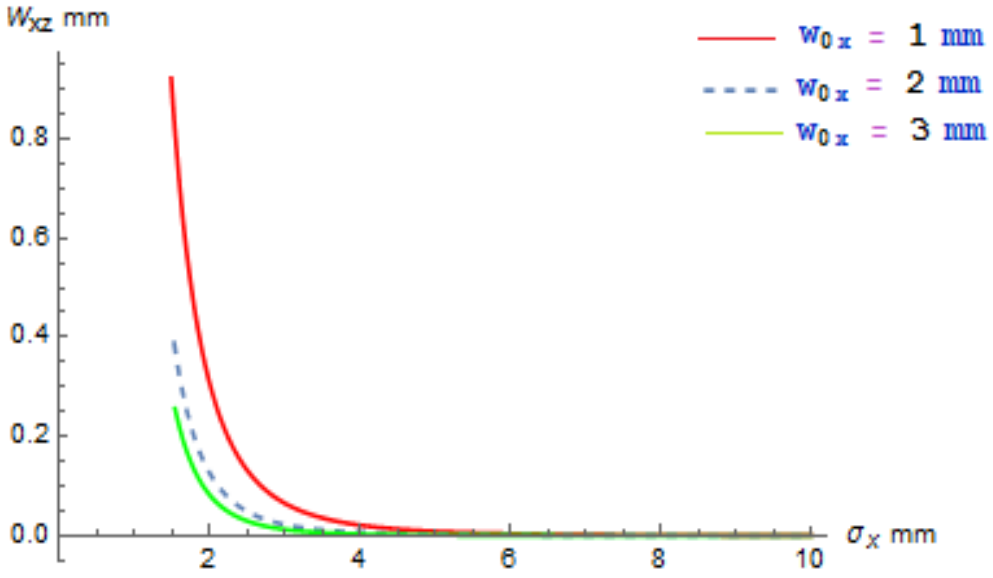

Figure 4.28 Effective Beam Size versus coherence length for partially coherent HGB in focal plane in x direction for w_0 = 2 mm.

In the figure 4.28 it is observed that Effective beam size has maximum value for smallest value of w_{0x} and as w_{0x} increases the rate of decrease of Effective beam size increases.

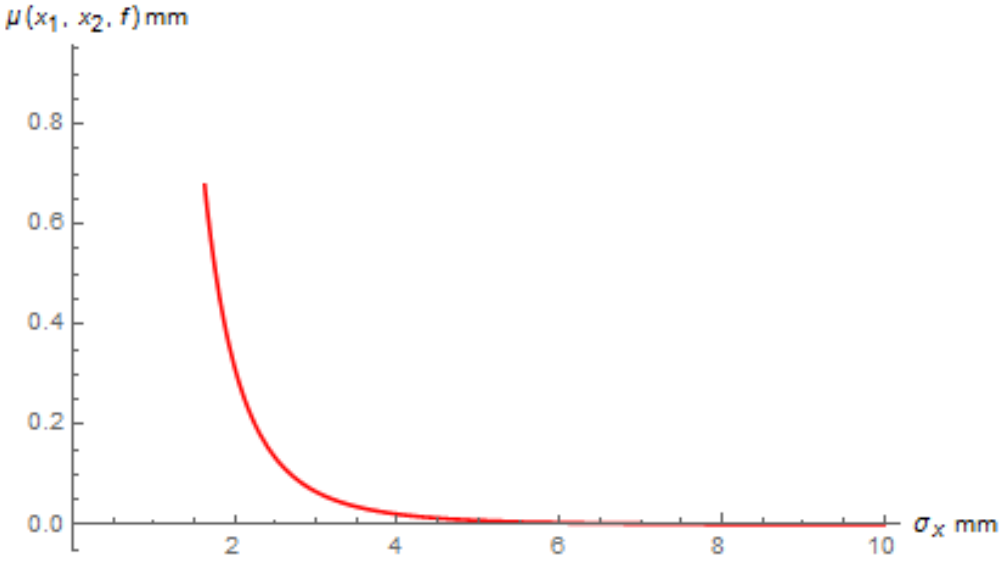

Figure 4.29 Effective Beam Size versus coherence length for partially coherent HGB in focal plane in x direction for w_0 = 1mm.

In figure 4.29 it is shown that the result obtained for w_0 = 1 mm has similar properties as obtained for w_{0x} = 1 mm but with lower maximum value of Effective beam size. The rate of decrease is also found out to be same.

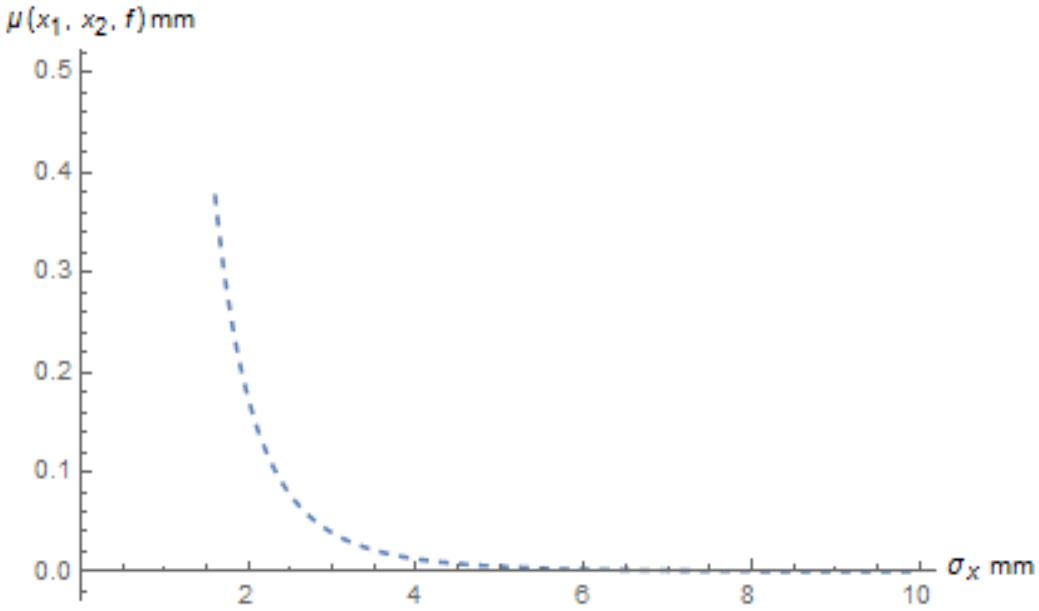

Figure 4.30 Effective Beam Size versus coherence length for partially coherent HGB in focal plane in x direction for w_0 = 2 mm.

It is clear from figure 4.30 that the result obtained for Effective beam size with w_0 = 2 mm is same as that for w_{0x} = 2 mm.

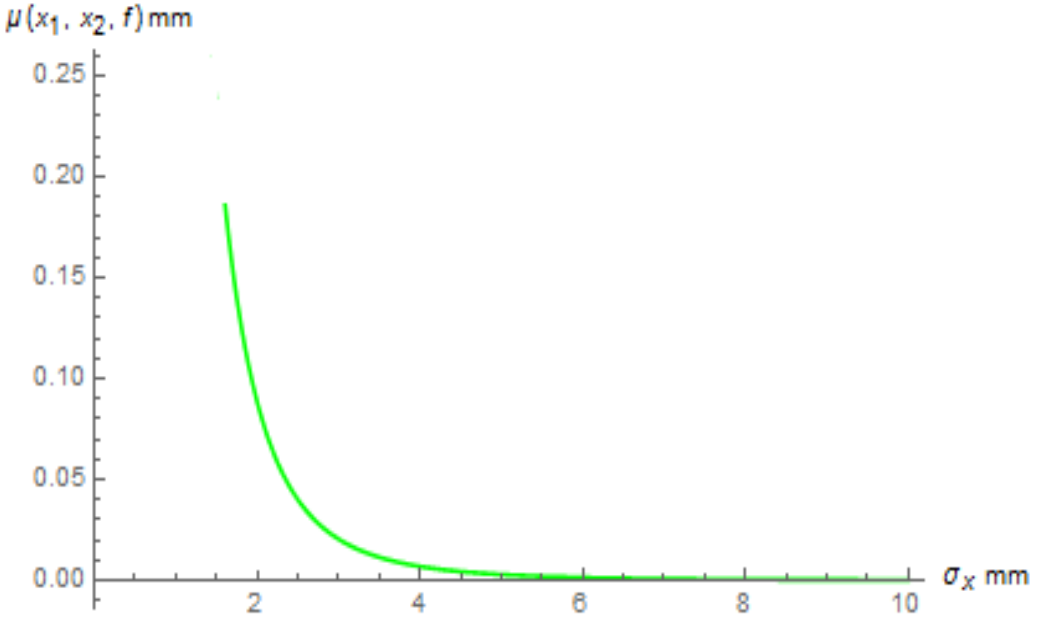

Figure 4.31 Effective Beam Size versus coherence length for partially coherent HGB in focal plane in x direction for w_0 = 3 mm.

It is evident from figure 4.31 that as value of w_0 increases the value of Effective beam size decreases and rate of its decrease increases.

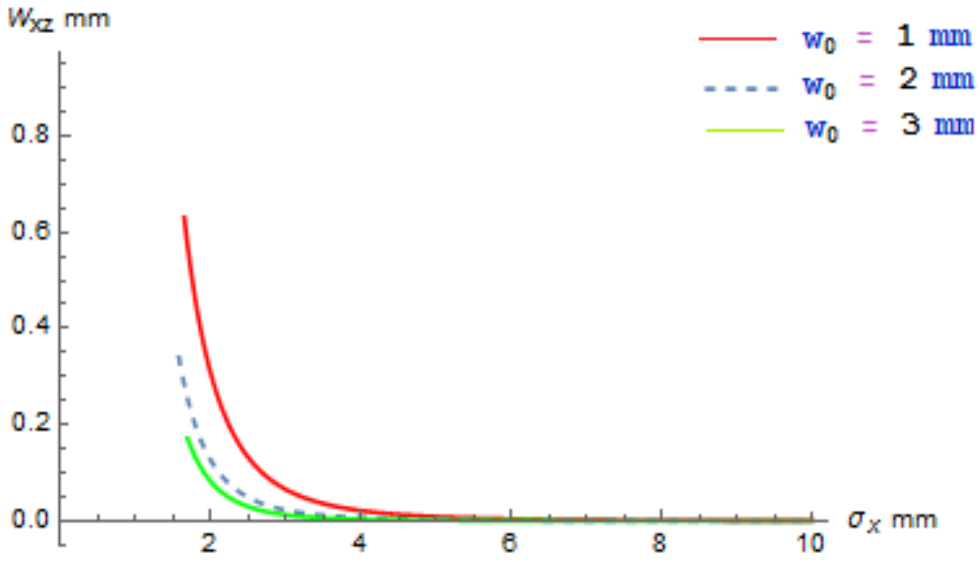

Figure 4.32 Effective Beam Size versus coherence length for partially coherent HGB in focal plane in x direction for w_{0x} = 2 mm.

In contrast to Lorentz-Gauss beams where there is a threshold point after which effective beam size is asymptotically increasing for Hermite-Gaussian beams there exists a threshold point after which effective beam size diminishes. The threshold point of coherence length for Hermite-Gaussian beam is obtained as 6mm from above results. For lower values of w_{0x} the maximum value of effective beam size is obtained and as the value of w_{0x} increases maximum value of effective beam size decreases. Rate of decrease of effective beam size is increasing with larger w_{0x}. Same is true for different values of w_0 but the maximum value of effective beam size is obtained with lowest value of w_{0x}.

CHAPTER 5

Conclusion and Future Scope

Conclusion

In this work we have compared the characteristics of Spatial complex degree of coherence and Effective beam size of Lorentz-Gauss and Hermite-Gaussian beams. We investigated case of unstable resonator. The transmission of two beams in paraxial ray matrix system is analyzed. The dependence of these two properties of beams on beam parameters and coherence length is shown and the role of *ABCD* parameters is widely discussed. We have drawn following conclusions from our analysis:

1.) The complex spatial degree of coherence does not saturate for maximum value 1 if the beam parameters are not much larger than the wavelength. It is evident from the results that larger w_0 and w_{0x} has larger complex spatial degree of coherence. Hence, focal length plays important role for the performance of Lorentz-Gauss beams.

2.) The value of complex spatial degree of coherence is 1 for Gaussian beam so it should be as near to 1 as possible for other beams too therefore we can conclude that if the ratio of beam parameters and wavelength is not significant than we should use optical beams for smaller values of w_0 and w_{0x}.

3.) As the complex spatial degree of coherence is same of these two beams they can be used for applications which need similar spatial degree of coherence closer to that of Gaussian beam and corresponding to the requirement of effective beam size any of the two beams can be used.

4.) We have found out in this work that for Effective beam size of Lorentz-Gauss beams there exists a threshold point between coherence length value of 0.1 mm to 2 mm after which effective beam size is asymptotically increasing.

5.) We have witnessed that for high gain Lorentz-Gauss beam larger Effective beam size is obtained at larger w_{0x} but the maximum value tends to saturate faster for higher values of $w_{0x.}$ The maximum value of Effective beam size is same for different values of w_0, which clearly shows that changing the value of w_0 does not show any significance in the maximum attainable Effective beam size by Lorentz-Gauss beam.

6.) We observed that for Hermite-Gaussian beams there exists a threshold point after which Effective beam size diminishes. The threshold point of Hermite-Gaussian beam is obtained for coherence length nearer to 6mm.

7.) In contrast to Lorentz-Gauss beam high gain Elegant Hermite-Gaussian beam attains larger Effective beam size at smaller values of w_0 and w_{0x}. It is also evident from the results that in this case changing the value of w_0 affects the Effective beam size equally but the maximum value of effective beam size is obtained with lowest value of w_{0x}.

Future Scope

The results obtained in this work will be of practical use in Optical communication at long distance.

- There is a scope to investigate the transmission of Lorentz-Gauss and Hermite-Gaussian beams through paraxial and complex ray matrix system.
- The properties of Lorentz-Gauss and Hermite-Gaussian beams can be studied in turbulent atmosphere for the case of unstable resonator.
- The properties of Lorentz-Gauss and Hermite-Gaussian beams can be investigated in anisotropic media for the case of unstable resonator.
- The approach used in this work can be extended in the field of photonics.

REFERENCES

[1]. Fundamentals of photonics. B. E. A. Saleh, M. C. Teich, *John Wiley & Sons*, 1991

[2]. Omar El Gawhary and Sergio Severini, "Lorentz beams and symmetry properties in paraxial optics", *J. Opt. A: Pure Appl. Opt.*, Vol. 8, pp. 409-414, 2006

[3]. G. Zhou, "Beam propagation factors of a Lorentz-gauss beam", *Springer*, Vol. 3, pp. 313-319, 2009

[4]. X. Chu et. al. "Average intensity and spreading of a Lorentz-Gauss beam in turbulent atmosphere", *Optics express*, Vol. 18, pp. 726-731, 2010

[5]. H. Kogelnik and T. Li, "Laser beams and resonators", *Appl. Opt.*, Vol. 5, pp. 1550-1567, 1966

[6]. S. Ramo et. al., "Fields and Waves in Communication Electronics", *Wiley*, 1965

[7]. W. Brouwer, "Matrix Methods in Optical Instrument Design", *Benjamin*, 1964

[8]. V. P. Byhov and L. A. Vainshtein, "Geometrical optics of open resonators", *Sov. Phys. - JETP*, Vol. 20, pp. 338-344, 1965

[9]. M. Bertolotti, "Matrix representation of the geometrical properties of open resonators", *Nuovo Cimento*, Vol. 32, pp. 1242-1257, 1964

[10]. W. K. Kahn, "Round table discussion on resonators", *Quasi Optics (Proc. Symposium on Quasi Optics), J. Fox, Ed., Polytechnic Press*, Polytechnic Institute of Brooklyn, pp. 397- 398, 1964

[11]. W. K. Kahn, "Geometric optical derivation of formula for the variation of the spot size in a spherical mirror resonator", *Appl. Opt.*, Vol. 4, pp. 758-759, 1965

[12]. W. K. Kahn and J. T. Nemit, "Ray theory of astigmatic resonators and beam waveguides", Symposium on Modern Optics, *J. Fox, Ed.*, Polytechnic Institute of Brooklyn, pp. 501-526, 1967.

[13]. N. Kurauchi and W. K. Kahn, "Rays and ray envelopes with stable optical resonators containing focusing media", *Appl. Opt.*, Vol. 5, pp. 1023-1029, 1966

[14]. D. Herriott et. al. "Paths in spherical mirror interferometers", *Appl. Opt.*, Vol. 3, pp. 523-526, 1964

[15]. H. Kogelnik,"Imaging of optical modes resonators with internal lenses", *Bell Sys. Tech. J.*, Vol. 44, pp. 455-494, 1965

[16]. A. Nussbaum, "Teaching of advanced geometrical optics", *Appl. Opt.*, Vol. 17, pp. 2128-2133, 1978

[17]. A. Gerrard and J. M. Burch, "Introduction to Matrix Methods in Optics", *Wiley*, 1975

[18]. G. W. Farnell, “Measured phase distribution in the image space of a microwave lens”, *Canad. J. Phys*., Vol. 36, pp. 935-942, 1958

[19]. R. W. Boyd, “Intuitive explanation of the phase anomaly of focused light beams”, *J. Opt. Soc. Am.*, Vol. 70, pp. 877-880, 1980.

[20]. P. Baues, “The connection of geometric optics with the propagation of gaussian beams and the theory of optical resonators”, *Opto-Electronics*, Vol. 1, pp. 103-118, 1969.

[21]. P. Baues, “Huygen’s principle in inhomogeneous isotropic media and a general integral equation applicable to optical resonators”, *Opto-Electronics*, Vol. 1, pp. 37-44, 1969.

[22]. S. A. Collins, Jr., “Lens-system diffraction integral written in terms of geometrical optics”, *J. Opt. Soc. Am*., Vol. 60, pp. 1168-1177, 1970.

[23]. F. Gori, “Matrix treatment for partially polarized, partially coherent beams,” *Opt. Lett.*, Vol 23, pp. 241–243, 1998

[24]. F. Gori, “Measuring Stokes parameters by means of a polarization grating,” *Opt. Lett.*, Vol 24, pp. 584–586, 1999

[25]. G. P. Agrawal and E. Wolf, “Propagation-induced polarization changes in partially coherent optical beams,” *J. Opt. Soc. Am. A*, Vol 17, pp. 2019–2023, 2000

[26]. F. Gori et. al., “Use of the van Cittert–Zernike theorem for partially polarized sources,” *Opt. Lett*., Vol 25, pp. 1291–1293, 2000

[27]. G. Gbur and D. F. V. James, “Unpolarized sources that generate highly polarized fields outside the source,” *J. Mod. Opt.*, Vol 47, pp. 1171–1177, 2000

[28]. F. Gori et. al.,“Coherent-mode decomposition of partially polarized, partially coherent sources,” *J. Opt. Soc. Am. A*, Vol 20, pp. 78–84, 2003

[29]. J. Tervo et. al, “Degree of Coherence for Electromagnetic Fields”, *Optics Express*, Vol. 11, pp. 1137- 1143,2003

[30]. Fundamentals of Photonics, 2nd Ed., B. E. A. Saleh, M. C. Teich, *John Wiley & Sons*, 2007

[31]. http://www.rp-photonics.com/coherence.html

[32]. http://media.wiley.com/product_data/excerpt/20/04713583/0471358320.pdf

[33]. H. Kogelnik and T. Li, “Laser Beams and Resonators”, *Appl. Opt.*, Vol. 5, pp. 1550-1567, 1966

[34]. http://www.rp-photonics.com/optical_resonators.html

[35]. http://www.optiqueingenieur.org/en/courses/OPIangM01C03/co/Contenu03html

[36]. Naqwi A and Durst F. “focusing of diode laser beams: a simple mathematical model”, *Appl. Opt.*, Vol. 10, pp. 1780-1785, 1990

[37]. Dumke W P. “The angular beam divergence in double hetrojunction lasers with very thin active regions”. *IEEE journal of Quantum Electronics*, Vol. 3, pp. 400-402, 1975

[38]. Jia Li et. al. .” Diffraction of Lorentz-gauss beam in uniaxial crystals: orthogonal to optical axis”, *Higher Education Press and Springer-Verlag Berlin Heidelberg*, Vol. 3, pp. 292-302, 2010

[39]. L. Mandel, E. Wolf. “Optical coherence and quantum optics”, *Cambridge university press*, 1995

[40]. G. Zhou. “Propagation of a partially coherent Lorentz-Gauss beam through a paraxial ABCD optical system”, *Optics Express*, Vol. 18, pp. 4637-4643, 2010

[41]. Yunfeng Jiang et. al. “Radiation force of highly focused Lorentz-Gauss beams on a Rayleigh particle”, *Optics Express*, Vol. 19, pp. 9708-9713, 2011

[42]. Xun Wang, et. al. “Nonparaxial propagation of Lorentz-Gauss beams in uniaxial crystal orthogonal to optical axis”, *Opt. Soc. of Am.*, Vol.31, pp. 872-877, 2014

[43]. G. Zhou “non-paraxial propagation of a Lorentz gauss beam”. *J. of Opt. Soc. of Am.*, Vol. 20, pp. 141-147, 2009

[44]. A. Keshavarz and G. Honarasa.**“**Propagation of Lorentz–Gaussian Beams in Strongly Nonlocal Nonlinear Media”, *Comm. in Theo. Phy.*, Vol. 61, pp. 241-245, 2014

[45]. G. Zhou, “Propagation of the kurtosis parameter of a Lorentz–Gauss beam through a paraxial and real ABCD optical system”, *J. of Opt.*, Vol. 13, pp. 403-412, 2011

[46]. Hong Yu et. al., “Nonparaxial Lorentz and Lorentz–Gauss beams”, *Optik*, Vol. 121, pp. 1455–1461, 2010

[47]. H. Laabs, “Propagation of Hermite-Gaussian-beams beyond the paraxial approximation”, *Opt. Comm.*, Vol. 147, pp. 1–4, 1998

[48]. G. Zhou, “Generalized M^2 factors of truncated partially coherent Lorentz and Lorentz Gauss beams”, *J. Opt.*, Vol. 12, pp. 1-6, 2010

[49]. G. Zhou, “Analytical vectorial structure of a Lorentz–Gauss beam in the far field”, *Appl. Phys. B*, Vol. 93, pp. 891–899, 2008

[50]. S. Saghafi and C.J.R. Sheppard, “The beam propagation factor for higher order Gaussian beams”, *Opt. Comm.*, Vol. 153, pp. 207–210, 1998

[51]. Ji X and Li X, "Directionality of Gaussian array beams propagating in atmospheric turbulence", *J Opt Soc Am A*, Vol. 26, pp. 236-43, 2009

[52]. E. HT, "Hermite cosine Gaussian laser beam and its propagation characteristics in turbulent atmosphere", *J Opt Soc Am A*, Vol. 22, pp. 1527-35, 2005

[53]. Hyo-Chang Kim and Yeon H. Lee "Hermite–Gaussian and Laguerre–Gaussian beams beyond the paraxial", *Opt. Comm.*, Vol. 169, pp. 9–16, 1999

[54]. Yuan Y et. al. "M^2 factor of coherent and partially coherent dark hollow beams propagating in turbulent atmosphere", *Optics Express*, Vol. 17, pp. 17344-56, 2009

[55]. Q. Cao and X. Deng, "Corrections to the paraxial approximation of an arbitrary free propagation beam", *J Opt Soc Am A*, Vol. 15, pp. 1144-1148, 1998

[56]. G. Zhou, "Focal shift of focused truncated Lorentz–Gauss beam", *J Opt Soc Am A*, Vol. 25, pp. 2594-2599, 2008

[57]. G. Zhou, "Fractional Fourier transform of Lorentz–Gauss beams", *J Opt Soc Am A*, Vol. 26, pp. 350-355, 2009

[58]. G. P. Agrawal and D. Pattanayak, "Gaussian beam propagation beyond the paraxial approximation", *J Opt Soc Am A*, Vol. 69, pp. 575-578, 1979

[59]. Riccardo Pratesi and Laura Ronchi, "Generalized Gaussian beams in free space", *J Opt Soc Am A*, Vol. 67, pp. 1274-1276, 1977

[60]. G. Zhou, "Non-paraxial propagation of a Lorentz–Gauss beam", *J Opt Soc Am B*, Vol. 26, pp. 141-147, 2009

[61]. G. Zhou, "Propagation of a partially coherent hollow vortex Gaussian beam through a paraxial ABCD optical system in turbulent atmosphere", *Optics Express*, Vol. 20, pp. 9897-9910, 2012

[62]. T. Takenaka et. al. "Propagation of light beams beyond the paraxial approximation", *J Opt Soc Am A*, Vol. 2, pp. 826-829, 1985

[63]. L. W. Davis, "Theory of electromagnetic beams", *Phys. Rev. A*, Vol. 19, pp. 1177-85, 1979

[64]. Y. Yuan et. al., "Average intensity and spreading of an elegant Hermite–Gaussian beam in turbulent Atmosphere", *Optics Express*, Vol. 17, pp. 11130-39, 2009

[65]. J. Yang et. al., "Focusing of diode laser beams: a partially coherent Lorentz model", *Proc. SPIE 6824*, Semiconductor Lasers and Applications III, 68240A, 2008

[66]. G. Zhou, "Investigation in the far field characteristics of Lorentz beam from the vectorial structure", *J. of Mod. Opt.*, Vol. 55, pp. 993-1002, 2008

[67]. Chengliang Zhao and Yangjian Cai, "Propagation of partially coherent Lorentz and Lorentz–Gauss beams through a paraxial ABCD optical system in a turbulent atmosphere ", *J. of Mod. Opt*., Vol. 12, pp. 810–818, 2011

[68]. B. Rose et. al., "Complex ABCD-matrices: A general Tool for Analyzing Arbitrary Optical Systems", *Optical Sensors and Microsystems,* Vol. 33, pp. 97-114, 2000

[69]. P. P. Schmidt, "A Method for the Convolution of Lineshapes which involve the Lorentz Distribution", *J. of Phy. B*, Vol. 9, pp. 2331–2339, 1976

[70]. I. S. Gradshteyn and I. M. Ryzhik, "Table of Integrals, Series, and Products", *Academic Press*, New York, 1980

List of Publications

- Nivedita Mishra, Hardeep Singh, "Analysis of spatial beam parameters of Lorentz-Gauss and Hermite-Gaussian Beams through a paraxial ABCD Optical System" in communication with *Microwave and Optical technology letters*.
- Nivedita Mishra, Hardeep Singh, "Analysis of spatial complex degree of coherence of Lorentz-Gauss Beams through a paraxial ABCD Optical System", *International Journal for Innovative Research in Science & Technology*, vol. 1, pp. 401-405, 2015
- Nivedita Mishra, Hardeep Singh, "Analysis of effective beam size of Lorentz-Gauss Beams through a paraxial ABCD Optical System", in OPTO-Meeting for Young Researchers & 10th Anniversary International SPIE Student Chapter Meeting 2015 conference, OPTO2015
- Nivedita Mishra, Hardeep Singh, "Analysis of spatial complex degree of coherence of Hermite-Gaussian Beams through a paraxial ABCD Optical System", accepted in *International Journal for Innovative Research in Science & Technology*.
- Hardeep Singh, Nivedita Mishra, "Performance Analysis of NRZ, RZ, Raised Cosine and Gaussian Modulation Formats in 32x10 Gbps WDM System with Different Compensation Techniques", accepted in "*Novel Optical Systems Design and Optimization XVIII" SPIE conference*, 2015.